Abstracts

Contributed Talks

Large magnetoresistance by Pauli blockade in hydrogenated graphene

J. Guillemette,[1] N. Hemsworth,[2] A. Vlasov,[2] J. Kirman,[2] F. Mahvash,[2,3] P. L. Lévesque,[4] M. Siaj,[3] R. Martel,[4] G. Gervais,[1] S. Studenikin,[5] A. Sachrajda,[5] and T. Szkopek[2]

[1] *Department of Physics, McGill University, Montréal, Québec, H3A 2A7, Canada*

[2] *Department of Electrical and Computer Engineering, McGill University, Montréal, Québec, H3A 2A7, Canada*

[3] *Department of Chemistry, Université du Québec à Montréal, Montréal, Québec, H3C 3P8, Canada*

[4] *Department of Chemistry, Université de Montréal, Montréal, Québec, H3C 3J7, Canada*

[5] *National Research Council Canada, 1200 Montreal Road, Ottawa, Ontario, K1A 0R6*

We report the observation of positive magnetoresistance in millimetre scale hydrogenated graphene with magnetic field oriented in the plane of the graphene sheet [1]. A positive, large magnetoresistance (LMR) in excess of 200% at a temperature of 300 mK and a field of 32 T was observed in this configuration, reverting to negative magnetoresistance with the magnetic field oriented normal to the graphene plane [2]. Positive LMR is absent in pristine millimetre scale graphene. Previous work by independent groups has shown that in-plane MR effects in graphene are comparatively small at a level of below 5% [3,4], with negligible in-plane MR observed in pristine graphene at in-plane magnetic fields of up to B = 30 T [5].

We attribute the positive, in-plane, LMR to Pauli-blockade of hopping conduction in accord with the theory of Kamimura et al. [6], developed further by Matveev at al. [7]. In contrast with the band conduction of pristine graphene, disorder introduced by hydrogenation imparts thermally activated hopping conduction. An in-plane magnetic field spin-polarizes the localized electrons participating in hopping conduction, thereby suppressing transitions forbidden by Pauli exclusion and increasing resistance. Notably, the atomic layer thickness (0.3 nm) of hydrogenated graphene suppresses magneto-orbital coupling in the in-plane geometry, thereby allowing the positive LMR of Pauli-blockade to be experimentally observed in a hopping conductor for the first time.

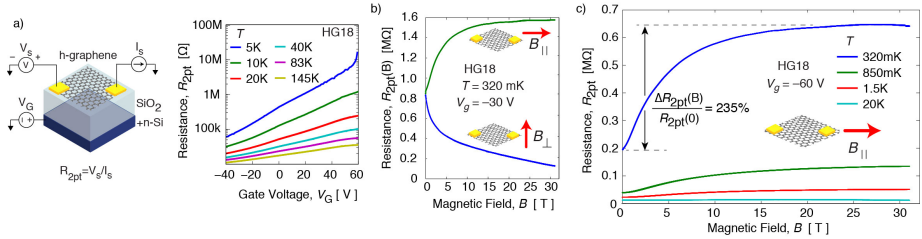

FIG. 1. *The measured 2-point resistance $R_{2\mathrm{pt}}$ of hydrogenated graphene sample (HG18) at zero magnetic field versus back-gate voltage V_G is plotted in a) at different temperatures T, showing insulating behaviour and hole conduction. b) The resistance $R_{2\mathrm{pt}}(B)$ of HG18 is plotted versus magnetic field B oriented in-plane, $B_{\parallel}$, and out-of-plane, $B_{\perp}$, to the graphene at $T = 320$ mK and $V_G = -30$ V. c) The temperature dependence of the resistance $R_{2\mathrm{pt}}(B)$ of sample HG18 is plotted versus in-plane field B at $V_G = -60$ V. A maximum magnetoresistance of $\Delta R_{2\mathrm{pt}}(B)/R_{2\mathrm{pt}}(0) = 235\%$ is observed.*

[1] J. Guillemette *et al.*, Large magnetoresistance by Pauli blockade in hydrogenated graphene, arXiv:1802.08295 [cond-mat.mes-hall].
[2] J. Guillemette *et al.*, Quantum Hall effect in hydrogenated graphene, Phys. Rev. Lett. **110**, 176801 (2013).
[3] M. B. Lundeberg and J. A. Folk, Rippled Graphene in an In-Plane Magnetic Field: Effects of a Random Vector Potential, Phys. Rev. Lett. **105**, 146804 (2010).
[4] H.-C. Wu *et al.*, Large positive in-plane magnetoresistance induced by localized states at nanodomain boundaries in graphene, Nature Comm. **8**, 14453 (2017).
[5] F. Chiappini *et al.*, Magnetotransport in single-layer graphene in a large parallel magnetic field, Phys. Rev. B **82**, 085302 (2010).
[6] H. Kamimura, A. Kurobe and T. Takemori, Magnetoresistance in Anderson-localized Systems, Physica B+C **117-118**, 652 (1983).
[7] K.A. Matveev, *et al.*, Theory of hopping magnetoresistance induced by Zeeman splitting, Phys. Rev. B **52**, 5289 (1995).

Chiral edge photogalvanic effect in graphene in the quantum Hall regime

M. V. Durnev,[1] S. A. Tarasenko,[1] H. Plank,[2] J. Pernul,[2] S. Candussio,[2] K.-M. Dantscher,[2] E. Mönch,[2] A. Sandner,[2] J. Eroms,[2] D. Weiss,[2] and S. D. Ganichev[2]

[1] *Ioffe Institute, St. Petersburg, Russia*

[2] *Terahertz Center, University of Regensburg, Regensburg, Germany*

We report on the observation of direct electric current flowing at the chiral edge channels in unbiased graphene caused by illumination of the sample edges with terahertz radiation. The chiral edge channels are formed in the presence of external magnetic field directed normally to graphene plane that drives the system in the quantum Hall regime. The observed photocurrent has opposite direction at opposite edges, but the same direction for electrons and holes. The direction of the photocurrent at a given edge is defined by the sign of external magnetic field, while its amplitude is controlled by the radiation polarization. We show that this behaviour is in strong contrast with the one of the edge photocurrent in the classical regime of low magnetic fields. In the latter case the edge photocurrent is caused by asymmetric scattering of charge carriers at the edges and changes its direction when the polarization of terahertz field is reversed.

The samples we use in our study are the Hall bars made of stacks of exfoliated graphene covered with hexagonal boron nitride. The carrier mobilities in these samples reach 7×10^4 cm^2/Vs and the carrier densities can be varied in a wide range by a back gate. Experiments were performed with a pulsed terahertz NH_3 gas laser operating at 3.3 THz. An external magnetic field was applied normal to the sample surface and parallel to the radiation (Faraday geometry) and all measurement were done at 4.2 K. Transport measurements demonstrated that the first plateau of the quantum Hall effect is reached at already 0.5 T.

We attribute the observed direct electric current in the graphene samples in the quantum Hall regime to the chiral edge photogalvanic effect. This effect is general for two-dimensional systems with free carriers in a strong out-of-plane magnetic field, when the chiral edge states are formed. The indirect (Drude-like) absorption of terahertz photon with energy smaller than the cyclotron gap results in generation of non-equilibrium electrons and holes within the chiral channel. Dispersion of the edge velocities of the photo-generated carriers leads to generation of dissipative contribution to the edge current, which can be measured experimentally. The suggested mechanism explains the main observations: the change of current direction under reversal of magnetic field sign, and the same current direction in electron and hole chiral channels. We develop microscopic theory of the chiral photogalvanic effect and calculate its polarization dependence. Theoretical results agree well with experimental data.

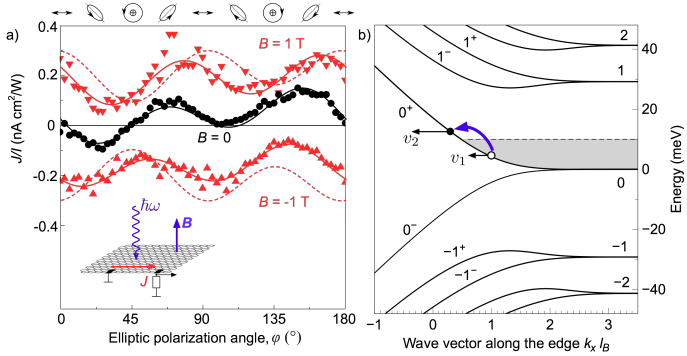

FIG. 1. *Experimental observation and mechanism of the edge photogalvanic effect in the quantum Hall regime. (a) Edge photocurrent as a function of elliptic polarization of THz electric field at zero magnetic field (circles) and magnetic field $B = \pm1$ T (triangles). Note that the photocurrent direction at $B \neq 0$ is controlled by the sign of B and not the polarization of the terahertz field. Solid lines are fits of experimental data by empirical formulae, dashed lines demonstrate theoretically predicted behaviour within the discussed mechanism. Inset shows the experiment geometry. (b) Schematic illustration of the photocurrent generation: The absorption of terahertz radiation leads to generation of non-equilibrium electrons and holes in the chiral edge channels and, hence, generation of electric current. Panel shows the spectrum of Landau levels in graphene with an armchair edge at $B = 1$ T, the dashed line illustrates the position of the Fermi level.*

Spin and Charge Transport in Few-Layer Graphene and Phosphorene

Chun Ning (Jeanie) Lau

Department of Physics, The Ohio State University, Columbus, OH 43210, USA

Low dimensional materials constitute an exciting and unusually tunable platform for investigation of integer and fractional quantum Hall states. Here I will present our results on transport measurements of high quality graphene and phosphorene devices. In trilayer and tetralayer graphene, we have observed Lifshitz transition and tunable symmetries of integer and fractional states[1, 2]. In few-layer black phosphorus devices with mobility up to 50,000 cm^2/Vs, integer QH states are resolved at a few Tesla, and fractional states at filling factor -4/3 and -0.56±0.1 are observed[3, 4]. Lastly, I will discuss our recent observation of robust long distance spin transport through the antiferromagnetic state in graphene.

Reference

1. Stepanov, P., et al., *Tunable Symmetries of Integer and Fractional Quantum Hall Phases in Heterostructures with Multiple Dirac Bands.* Physical Review Letters, 2016. **117**(7): p. 076807.
2. Shi, Y., et al., *Tunable Lifshitz Transitions and Multiband Transport in Tetralayer Graphene.* Physical Review Letters, 2018. **120**(9): p. 096802.
3. Tran, S., et al., *Surface transport and quantum Hall effect in ambipolar black phosphorus double quantum wells.* Science Advances, 2017. **3**(6): p. e1603179.
4. Yang, J., et al., *Integer and Fractional Quantum Hall effect in Ultra-high Quality Few-layer Black Phosphorus Transistors.* Nano Letters, 2018. **18**: p. 229.

Proximity Effects in Graphene/α-$RuCl_3$ Heterostructures

Boyi Zhou,[1] Paige Lampen-Kelley,[2] David Mandrus,[2] Stephen Nagler,[2] and Erik Henriksen[1]

[1]*Dept. of Physics, Washington University in St. Louis, St. Louis, MO, USA*

[2]*Oak Ridge National Laboratory, Oak Ridge, TN, USA*

Bulk crystals of the layered antiferromagnetic Mott insulator α-$RuCl_3$ have recently been found to exhibit features related to the Kitaev quantum spin liquid; quantum critical behavior has been described when ~ 8 T in-plane magnetic fields quench the long-range magnetic order [1,2]. Excitations of this Kitaev QSL are expected to show Majorana or non-Abelian features. Since the QSL phase is nominally a two-dimensional phenomenon, it may be possible to stabilize it in its single- or few-layer form. We have mechanically exfoliated α-$RuCl_3$, readily achieving monolayers that are stable in air for months [3]. Raman spectroscopy has revealed a structural distortion in mono- and bi-layers, and DC transport shows insulating behavior down to 35 K. To access the low temperature regime, we fabricated van der Waals heterostructures consisting of α-$RuCl_3$ flakes placed on graphene Hall bars. The graphene resistivity acquires an unusual temperature dependence with a kink between 10-20 K, close to the Néel temperature at which antiferromagnetic ordering occurs in α-$RuCl_3$. Subtracting the impurity and phonon contributions, the remnant resistivity is seen to spike at $T_{Néel}$ and then fall off with increasing temperature. In an in-plane field the remnant resistivity increases; while a perpendicular field induces an apparent splitting of the graphene $N = 0$ Landau level. Together these illustrate that transport in graphene is significantly impacted by proximity to α-$RuCl_3$. These α-$RuCl_3$-based devices may offer a new route toward studying quantum spin liquid phenomena and topological excitations in 2D materials.

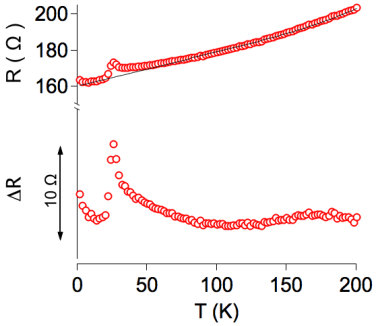

FIG. 1. *Top: Graphene/α-$RuCl_3$ Hall bar resistance vs temperature, with black line showing phonon contribution. Bottom: remnant resistance due to interaction of graphene and α-$RuCl_3$ flake.*

[1] Baek, S. H., *et al.* Phys. Rev. Lett. **119**, 037201 (2017).

[2] Zheng, J., *et al.* Phys. Rev. Lett. **119**, 227208 (2017).

[3] Zhou, B, Henriksen E., *et al.*, J. Phys. Chem. Sol. *online proof* (2018).

Thickness and gate-voltage dependence on magnetic-field induced phase transition in graphite

Toshihiro Taen,[1] Kazuhito Uchida,[1] and Toshihito Osada[1]

[1] *Institute for Solid State Physics, The University of Tokyo, Kashiwa, Chiba, Japan*

Magnetic-field induced phase transition in graphite recently regains much attention. However, the origin of a semimetal-insulator transition at $B \simeq 30$ T is still not clear. Although an exotic density-wave state, *valley-density wave* state, is theoretically proposed, experimental verification was a challenging problem. In order to identify the electronic state of the insulator phase, we investigated the phase transition in thin-film graphite samples that were fabricated on silicon substrate by mechanical exfoliation method. By observing in-plane resistance under pulsed magnetic field up to 40 T, we found that the critical magnetic field of the phase transition can be controlled by the thickness. Figure 1(a) is the phase transition lines for samples with different thickness. The phase transition line shifts higher and temperature dependence of it becomes smaller by reducing thickness. This is in contrast with the result in the swift neutron irradiated graphite, where the transition line shifts almost in a parallel manner with the introduction of disorders [1]. These trends are qualitatively reproduced by the density-wave model by introducing a quantum size effect. In the thick enough system, (i.e., bulk), as illustrated in Fig. 1(b), the dispersion is continuous, while that in the thin-film sample is discrete owing to the quantum seize effect, as shown in Fig. 1(c). The density-wave state is realized when a pair of states at k_z and $k_z + q_z$ just at the Fermi level gives a large contribution on the density-response function $\chi(\mathbf{q})$. Here q_z is related to the characteristic length of the density wave. However, in thin-film system, such pairs cannot be found in some cases owing to the sparse k_z. Moreover, the energy-level spacing gives rise to the small temperature dependence. Owing to these kinds of sparseness, the density-wave state becomes unstable in thin-film system, which is in good agreement with our experimental findings. Therefore, we strongly suggest that the insulating state appearing at $B \simeq 30$ T is the density-wave state.

In addition to the thickness dependence, we also study the gate-voltage dependence in field-effect transistor of thin-film graphite. In this study, we applied the magnetic field up to 35 T in DC field facility of the National High Magnetic Field Laboratory. Under zero magnetic field, the gate-voltage dependence is absent in the in-plane resistance. By contrast, the magnetoresistance has a strong gate-voltage dependence. On the other hand, the critical field of the semimetal-insulator transition is weakly dependent on the gate voltage. These gate-voltage dependences should be explained by the band-bending and carrier doping effects.

A portion of this work was performed at the National High Magnetic Field Laboratory, which is supported by National Science Foundation Cooperative Agreement No. DMR-1157490 and the State of Florida, and by JSPS KAKENHI — "Fund for the Promotion of Joint International Research" Grant Number JP15K21722.

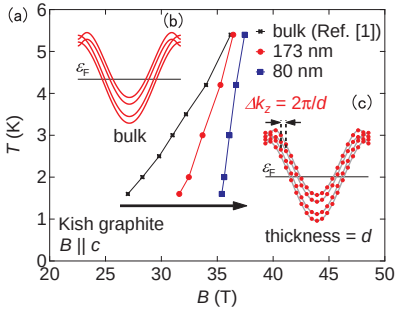

FIG. 1. *(a) Semimetal-insulator phase transition line of 173- and 80-nm-thick thin-film graphite in temperature and magnetic-field phase diagram. By reducing the thickness, the transition line shifts higher and reduces temperature dependence. These trends can be understood by a density-wave model by introducing a quantum size effect. In the thick-enough system (i.e., bulk), the dispersion of the Landau subband is continuous (b), while the interval of reciprocal lattice points, expressed as $\Delta k_z = 2\pi/d$ (d is thickness), is discrete in thin-film system (c). Owing to this discreteness, the density-wave state becomes unstable, which is consistent with the experimental observation.*

[1] H. Yaguchi *et al.* J. Phys. Soc. Jpn. **68**, 1300 (1999).

Coupling between quantum Hall edge channels across bulk two-dimensional electron systems

Ngoc Han Tu[1], Masayuki Hashisaka[1,2], Takeshi Ota[1], Yoshiaki Sekine[1], Koji Muraki[1], Toshimasa Fujisawa[2], and Norio Kumada[1]

[1] *NTT Basic Research Laboratories, NTT Corporation, 3-1 Morinosato-Wakamiya, Atsugi, 243-0198, Japan*
[2] *Department of Physics, Tokyo Institute of Technology, 2-12-1 Ookayama, Meguro, Tokyo 152-8551, Japan*

In an integer quantum Hall (QH) state, electrons propagate in one-dimensional (1D) edge channel along the periphery of the two-dimensional electron system (2DES). These chiral edge channels (ECs) are considered as ideal ballistic one-dimensional channels, which open the way to investigate electron quantum optics on electronic interferometers. In contrast to the case of photons, the Coulomb interaction plays a major role for electron dynamics in ECs. For instance, interactions between electrons in adjacent ECs induces decoherence and energy relaxation. Two coupled ECs are also used to investigate properties of Tomonaga-Luttinger liquid, the model to describe interacting electrons in 1D system. On the other hand, interaction between ECs on opposite sides of a sample is usually ignored because of a large distance. However, a recent report using a system composed of two ECs separated by etching has demonstrated that interaction strength between ECs obeys the logarithmic law with the distance and is not negligible even at a distance of 50 μm [1].

Here, we report an observation of the coupling between ECs along opposite sides of a graphene Hall bar device in the integer QH effect regime via high-frequency transport measurements. We used graphene grown on SiC. The graphene sample has a bar shaped region with a width of 50 μm and a length of 350 μm [Fig. 1(a)]. A charged wavepacket was excited in one EC (EC1), and the time-dependent current in ECs (EC1 and EC2) on both sides of the device was detected through two ohmic contacts, Det1 and Det2, placed at the downstream of EC1 and EC2, respectively. The finite current appears at both Det1 and Det2, demonstrating the existence of the coupling between ECs. In the QH state at the filling factor $\nu = 2$, the current at Det1 shows a peak, while that at Det2 shows a peak followed by a dip [Fig. 1(b)]. This can be explained by the capacitive coupling across the 50-μm-wide incompressible bulk. The amplitude of the current at Det2 is as large as 20% of that at Det1, much larger than naively expected. On the other hand, in a non-QH state, a single peak appears both at Det1 and Det2 [Fig. 1(c)]. This behavior is as expected for the conductive coupling through the compressible bulk. Interestingly, we found that even inside the QH state, the strength of the capacitive coupling varies with magnetic field B. As B is decreased to the boundary with the non-QH state ($B = 1.6$ T), the amplitude of the peak and dip in the current at Det2 increases, indicating the strengthening coupling. We suggest that the presence of localized states inside the incompressible bulk enlarge the coupling strength. We obtained consistent results in GaAs/AlGaAs sample. Our results clarify the existence of the coupling of ECs on opposite side of a typical QH device, and suggest that the coupling has to be taken into account to better understand quantum transport in ECs.

[1] P. Brasseur et al., Phys. Rev. B 96, 081101(R), (2017).

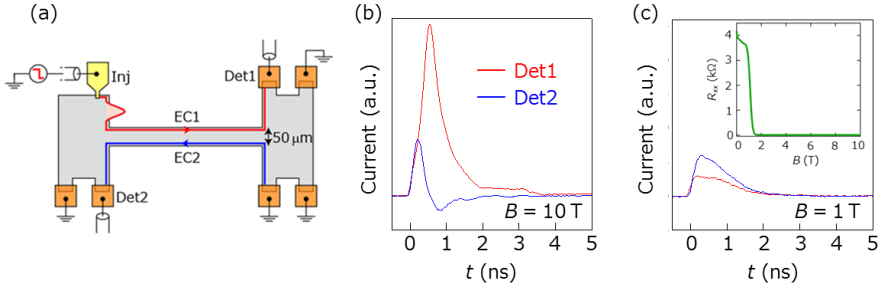

FIG. 1. (a) Schematic of a graphene sample. An injection gate (yellow) and ohmic contacts (orange) are patterned on graphene (grey). High-frequency lines are connected to the injection gate and two ohmic contacts labelled Det1 and Det2. (b) Current at Det1 and 2 as a function of t at $B = 10$ T, deep inside the QH state. (c) Current at Det1 and 2 as a function of t at $B = 1$ T, in the non-QH state. Inset shows R_{xx} as a function of B.

Observation of interlayer anyon pairing through fractional quantum Hall drag

Xiaomeng Liu,[1] Zeyu Hao,[1] Jia Li,[2] Kenji Watanabe,[3] Takashi Taniguchi,[3] Cory Dean,[2] Bertrand Halperin,[1] and Philip Kim[1]

[1]*Department of Physics, Harvard University, USA*

[2]*Department of Physics, Columbia Univeristy, USA*

[3]*National Institute for Material Science, Japan*

In an electron double-layer system, interlayer Coulomb interaction can induce novel emergent phases such as exciton condensate. The interlayer interaction effect can be further enhanced by strong magnetic fields, which quenches the kinetic energy through Landau quantization. We study Coulomb drag in strongly coupled graphene double-layer systems with small interlayer separation under strong magnetic fields. Besides exciton condensate states, we observed signatures of interlayer correlation at fractional filling factors. When both layers are ν=2/5 filled, we observed quantized Hall resistance of $1.5h/e^2$ in the drive layer and quantized Hall drag of h/e^2. While imbalanced, the Hall drag quantization persists if for each electron added onto one layer, 2/3 of an electron charge is removed from the other layer. At extreme imbalance, this state is established by adding electrons to an empty layer while creating 2/3e charged quasi-particles (anyons) of 2/3 fractional quantum Hall state in the other layer. The Coulomb drag measurements suggest interlayer pairing between quasi-electrons in one layer and 2/3e anyons in the other layer. When equally filled, the state can be interpreted as (221) fractional interlayer correlated state, in which each electron bound with two magnetic flux from the same layer and one magnetic flux from the opposite layer. Our experiments demonstrate fascinating new phases formed by pairs of fractional charged anyons.

Exciton Rydberg States & Dielectric Environment Effects in Monolayer Semiconductors: Insight from High Magnetic Fields

Andreas Stier[1], Nathan Wilson[2], Junichiro Kono[3], Xiaodong Xu[2], and Scott Crooker[1]

[1] *National High Magnetic Field Lab, Los Alamos National Lab, Los Alamos, NM 87545*

[2] *Department of Physics, University of Washington, Seattle, WA 98195*

[3] *Department of Physics, Rice University, Houston, TX*

Excitons in atomically-thin semiconductors necessarily lie close to a surface, and therefore their properties are expected to be strongly influenced by the surrounding dielectric environment. However, systematic studies exploring this role are challenging, in part because the most readily accessible exciton parameter—the exciton's optical transition energy—is largely *un*affected by the surrounding medium. In this work we show that the significant role of the dielectric environment on 2D materials can be directly revealed through its systematic influence on the *size* of the exciton, which can be measured via the diamagnetic shift of the exciton transition in high magnetic fields [1, 2].

Using exfoliated WSe_2 monolayers affixed to single-mode optical fibers, we tune the surrounding dielectric environment by encapsulating the flakes with different materials [2] and perform polarized low-temperature magneto-absorption studies to 65 T. The systematic increase of the exciton's size with dielectric screening, and concurrent reduction in binding energy (also inferred from these measurements), is quantitatively compared with leading theoretical models based on the Keldysh potential for 2D materials. These results demonstrate how exciton properties -- and also the free-particle bandgap -- can be tuned in 2D van der Waals heterostructures via the surrounding dielectric environment. We also present recent 65 T measurements of high-quality hBN/WSe_2/hBN structures that permit an unambiguous identification and quantification of excited *1s*, *2s*, *3s*, and *4s* Rydberg states of neutral excitons [3]. The distinct diamagnetic shifts of these exciton Rydberg states (see Figure 1 below) allows not only for a quantitative comparison of experimental data with theoretical models for the attractive electron-hole potential in a 2D semiconductor, but most importantly also allows a direct measurement of exciton's reduced mass.

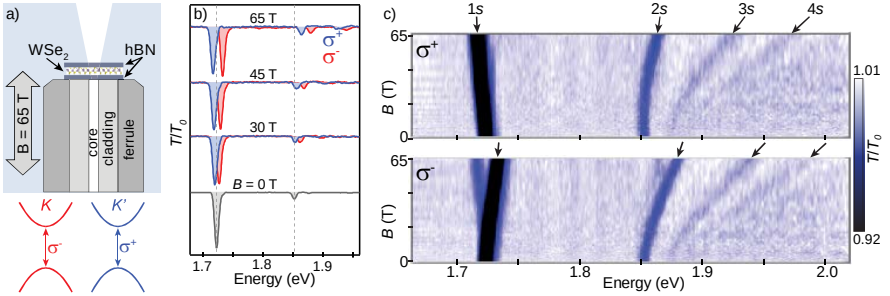

Figure 1: Polarized optical spectroscopy of hBN-encapsulated monolayer WSe_2 to 65 T, showing the distinct diamagnetic energy shifts of the *1s*, *2s*, *3s*, and *4s* Rydberg excitons, from which the exciton's reduced mass can be directly determined. Figure from Ref. [3].

[1] A. V. Stier *et al.*, *Nature Communications* **7**, 10643 (2016).
[2] A. V. Stier *et al.*, *Nano Letters* **16**, 7054 (2016).
[3] A. V. Stier *et al.*, *Physical Review Letters* **120**, 057405 (2018).

Magnetoinduced photocurrents in Weyl semimetals

L. E. Golub,[1] E. L. Ivchenko,[1] and B. Z. Spivak[2]

[1] *Ioffe Institute, St. Petersburg 194021, Russia*

[2] *University of Washington, Seattle, WA 98195, USA*

Weyl semimetals represent materials allowing for a solid-state realization of three-dimensional massless fermions with a linear energy dispersion and a definite chirality. The remarkable properties of Weyl semimetals are the chiral anomaly leading to a negative magnetoresistance, magnetic monopole in the momentum space with a nonzero Berry curvature and topologically induced surface Fermi arcs. In the present work, the magneto-gyrotropic photogalvanic effect (MPGE) in Weyl semimetals is studied. MPGE is an appearance of a photocurrent under unpolarized excitation in a magnetic field which flows backwards with the field reversal. The MPGE current density is related with the magnetic field $\boldsymbol{B}$ and the light intensity I as $\boldsymbol{j} = \chi I \boldsymbol{B}$, where χ is an even function of the magnetic field [1].

In a quantizing magnetic field, the energy spectrum of a Weyl semimetal consists of one chiral subband and a series of the valence (v) and conduction (c) magnetic subbands enumerated by the positive integer $n = 1, 2\ldots$, Fig. 1(a), with a dispersion dependent on the wavevector k directed along $\boldsymbol{B}$. We investigate the MPGE current injected by direct optical transitions between the valence and conduction magnetic subbands in a given Weyl node with the chirality $\mathcal{C} = \pm 1$. Due to the terms odd both in k and $\boldsymbol{B}$, the probability rates are asymmetric with a predominance of states with $\mathcal{C}kB > 0$ for the transitions $v, n \to c, n+1$ and $\mathcal{C}kB < 0$ for the transitions $v, n+1 \to c, n$. In these two kinds of transitions the electron energies of the initial and final states differ by $\hbar\omega_c^2/\omega$, where ω is the light frequency and the cyclotron frequency is $\omega_c = v_0\sqrt{2|eB|/\hbar c}$ with v_0 being the velocity of Weyl fermions. As a result, the final states' equilibrium occupations are different which gives rise to the MPGE current, Fig. 1(a). We have analyzed three frequency ranges, namely, $\omega > \omega_c(\sqrt{2}+1)$; $\omega_c(\sqrt{2}+1) > \omega > \omega_c$ and $\omega_c > \omega$ and found restrictions imposed by the level of chemical potential at zero temperature on the spectral intervals where the MPGE current is generated. The temperature smooths out the edges of these intervals. A value of the photocurrent is particularly high if one of the photocarriers is excited to the chiral subband with the energy below the cyclotron energy, Fig. 1(b). The derived expressions for the MPGE current are different in sign for monopoles of opposite chirality $\mathcal{C}$. We demonstrate that account for the tilt terms in the Hamiltonian results in the larger optical transition rate in the Weyl node with the chirality $\mathcal{C} > 0$ than in the node with $\mathcal{C} < 0$. This gives rise to the net MPGE current in multi-valley semimetals of the C_{2v} symmetry [2].

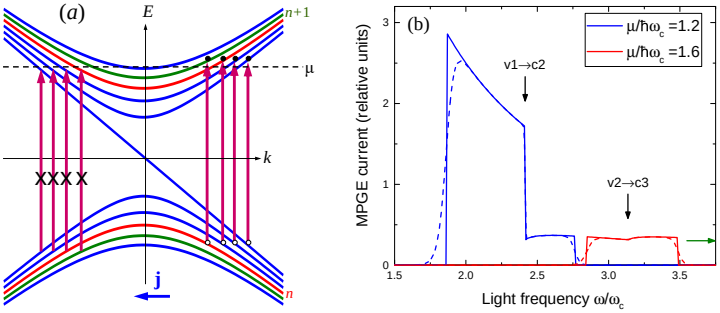

FIG. 1. *(a): Scheme of direct optical transitions between the one-dimensional subbands in a quantized magnetic field in the case $\mathcal{C}B > 0$. The transitions $v, n \to c, n+1$ result in the MPGE current since the $v, n+1 \to c, n$ transitions are blocked (crosses) by the Pauli principle. For $n \neq 0$ each transition occurs at two points k of opposite signs. The arrows illustrate the optical transitions, their starting points (open circles) are chosen at the side with the more probable transition rate. (b): Frequency dependence of the MPGE current calculated for two values of the chemical potential μ. Solid and dashed curves are calculated for zero temperature and $T = 0.01\hbar\omega_c$, respectively. The horizontal arrow shows the universal photocurrent value for high frequencies $\omega \gg \omega_c$.*

[1] L. E. Golub, E. L. Ivchenko, and B. Z. Spivak, JETP Lett. **105**, 782 (2017).

[2] L. E. Golub and E. L. Ivchenko, submitted to Phys. Rev. B

Quantum oscillations revealed in torque magnetometry and transport originating from magnetic breakdown in the nodal line semi-metal ZrSiS

T. Khouri,[1] M.R. van Delft,[1] S. Pezzini,[1] C.S.A Müller,[1] L. Schoop,[2] B. Lotsch,[2] M. I. Katsnleson,[3] A. Carrington,[4] N.E. Hussey,[1] and S. Wiedmann[1]

[1] *High Field Magnet Laboratory (HFML-EMFL), Radboud University, Toernooiveld 7, Nijmegen 6525 ED, Netherlands.*

[2] *Max Planck Institute for Solid State Research, Heisenbergstr. 1, 70569 Stuttgart, Germany.*

[3] *Institute for Molecules and Materials, Radboud University Nijmegen, 6525 ED Nijmegen, The Netherlands.*

[4] *H. Wills Physics Laboratory, University of Bristol, Tyndall Avenue, Bristol BS8 1TL, UK.*

ZrSiS is a material that belongs to the class of nodal line semi-metals (NLSMs) in which the conduction and valence band touch each other along a closed trajectory inside the Brillouin zone. Among all NLSMs, ZrSiS is considered to an almost ideal system as *all* energy bands that cross the Fermi energy have a Dirac like character in a range of ~ 2 eV around E_F [1].

We present a quantum oscillation study up to 33 T in high quality crystals of ZrSiS using magneto-transport (Shubnikov-de Haas effect) and torque magnetometry (de Haas-van Alphen effect). An example for the de Haas-van Alphen oscillations is shown in Figure 1 a) at 1.35 K. Apart from quantum oscillations that occur because of the closed orbits around the electron and holes pockets at the Fermi-surface, we observe oscillations that likely originate from magnetic breakdown when the momentum gap between adjacent electron and hole pockets is breached at sufficiently large magnetic fields.

With a Fast Fourier Transform (FFT) analysis, we identify several peaks at low frequencies f <1 kT and high frequencies in the region between 7.9 and 12 kT that originate from this phenomenon. The high-frequency part is illustrated in Figure 1 b). These magnetic breakdown related peaks in the FFT spectrum are most prominent when the magnetic field B is aligned parallel to the c-axis of the crystal and vanish rapidly under small tilt angles due to an increase of the breakdown gap between adjacent pockets, see Figure 1 a).

Intriguingly, the temperature dependence of the high-frequency oscillations in *magneto-transport* shows an anomalous damping and they survive up to several tenth of Kelvin [2]. We will present similarities and differences of the high frequency oscillations in both techniques to explore possible origins for this peculiar behaviour.

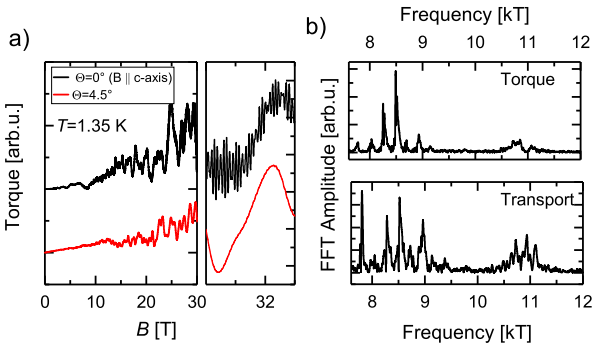

FIG. 1. *a) Angle dependence of the quantum oscillations measured in torque magnetometry at 0.35 K. The high frequency oscillations vanish under small tilt angles. b) FFT spectrum of the high frequency part in the region between 7.6 and 12 kT*

[1] L.M. Schoop *et al.*, Nat. Commun. **7**, 11696 (2016).
[2] S. Pezzini*et al.*, Nature Physics **14**, 178183 (2018).

Landau level spectroscopy of coupled Weyl points: a case study of semimetal NbP

Y. Jiang[1,2], S. Moon[2,3], Z. L. Dun[4], H. D. Zhou[4], M. Ozerov[2], Z. Jiang[1], D. Smirnov[2]

[1] *School of Physics, Georgia Institute of Technology, Atlanta, Georgia 30332, USA*

[2] *National High Magnetic Field Laboratory, Tallahassee, Florida 32310, USA*

[3] *Department of Physics, Florida State University, Tallahassee, Florida 32306, USA*

[4] *Department of Physics and Astronomy, University of Tennessee, Knoxville, Tennessee 37996, USA*

Recently, Weyl semimetal (WSMs) have attracted great attention in the search of three-dimensional zero-gap materials with non-trivial topology. In a WSM, the conduction band and valence band touch at isolated points in momentum space - Weyl points (WPs). In the vicinity of WPs, the electronic band structure can be described by an effective Hamiltonian resembling the Weyl equation in high energy physics. Consequently, the electrons in WSMs not only exhibit a linear dispersion but also carry chirality, giving rise to many exotic physics such as the Fermi arcs or the chiral anomaly [1].

The WPs always come in pairs and the coupling between the two WPs can significantly modify the band dispersion. Specifically, when the linear band from each WP overlaps, the band symmetry is reduced from the spherical symmetry of isolated WP to the axial symmetry of two coupled WPs. Band hybridization and avoided level crossing are also expected to occur. Recent studies have suggested that such a band modification is responsible for the breakdown of chiral anomaly and the opening of a notable band gap at high magnetic fields [2,3].

NbP is a member of the best-known WSM family, nonmagnetic transition-metal monopnictides (TX: T=Ta, Nb; X=As, P), hosting 12 pairs of WPs in the first Brillouin zone. Here, via combining theoretical calculations and infrared magneto-spectroscopy, we demonstrate the essential role of the coupling effect between two WPs in NbP. Both Faraday and Voigt geometries are investigated. We show that when the magnetic field is applied perpendicular to the separation of the CWPs, the symmetry of the system is reduced, leading to a field-induced band gap opening as well as coupling-induced LL crossings/anticrossings. Magnetic field dependence of the observed inter Landau level transitions deviates significantly from the expectation of isolated WPs, but can be well reproduced within the model of CWPs. Therefore, coupling between Weyl points should be considered as the basis for analysis of realistic WSMs.

[[1] N.P. Armitage, E. J. Mele, A. Vishwanath. Weyl and Dirac Semimetals in Three Dimensional Solids. arXiv:1705.01111 (2017)
[2] Chan, C.-K. & Lee, P. A. Emergence of gapped bulk and metallic side walls in the zeroth Landau level in Dirac and Weyl semimetals. Phys. Rev. B 96, 195143 (2017).
[3] Ramshaw, B. J. et al. Unmasking Weyl fermions using extreme magnetic fields. arXiv:1704.06944 (2017).

Electron-hole tunneling in the nodal line semi-metal HfSiS revealed by quantum oscillations

M.R. van Delft,[1] S. Pezzini,[1] T. Khouri,[1] C.S.A. Müller,[1] L. Schoop,[2] B. Lotsch,[2] A. Carrington,[3] N.E. Hussey,[1] and S. Wiedmann[1]

[1] *High Field Magnet Laboratory (HFML-EMFL), Radboud University, Toernooiveld 7, Nijmegen 6525 ED, Netherlands.*

[2] *Max Planck Institute for Solid State Research, Heisenbergstr. 1, 70569 Stuttgart, Germany.*

[3] *H. Wills Physics Laboratory, University of Bristol, Tyndall Avenue, Bristol BS8 1TL, UK.*

Nodal line semi-metals (NLSMs) belong to the class of topological semi-metals. In contrast to Dirac and Weyl semi-metals with nodal points in momentum space that are topologically protected by crystal symmetries, in NLSMs the valence and conduction bands touch each other along a closed one-dimensional trajectory inside the Brillouin zone [1].

We present a magneto-transport study on single crystals of the NLSM HfSiS up to 31 T. We observe pronounced quantum oscillations that are superimposed on a positive magneto-resistance [Figure 1a) at 1.3 K]. The corresponding Fast Fourier Transform (FFT) analysis is shown in Figure 1b). We discover two kinds of quantum oscillations: the first kind originates from individual closed orbits around an electron or hole pocket of the Fermi surface labeled as β (electron) and α (hole) pocket, respectively, which appear as the dominant peaks in the FFT. The second kind originates from magnetic breakdown and we identify as the 'figure of eight' orbit [2] defined by a trajectory enclosing adjacent β and α pockets with a frequency $\beta - \alpha$ [2,3] that occurs due to tunneling of charge carriers between electron and hole pockets across gaps in momentum space in the Z-R-A plane. In case the magnetic field B is slightly tilted away from the c-axis, this frequency vanishes due to the increase of the gap between the pockets in momentum space [4].

In addition, we observe high-frequency oscillations shown in Figure 1c) due to tunneling across all energy gaps in the Z-R-A plane similar to the sister compound ZrSiS [4] despite a larger spin-orbit coupling and consequently larger gaps in momentum space found in calculations using Density Functional Theory.

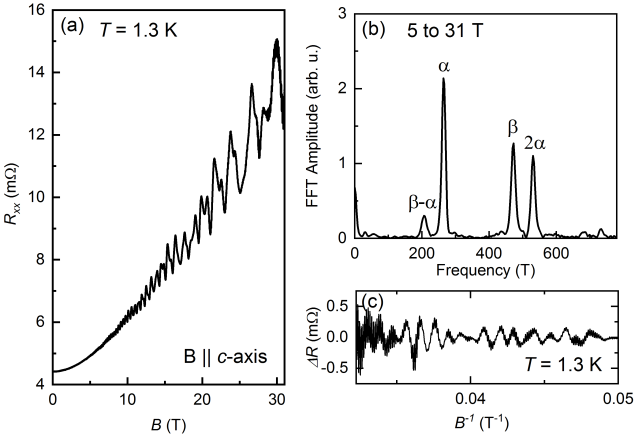

FIG. 1. *a) Longitudinal resistance R_{xx} as a function of magnetic field at 1.3 K for $B \parallel c$. b) Fast Fourier Transform of a) revealing the electron β and α hole pocket, and the 'figure of eight' orbit $\beta - \alpha$. c) High frequency oscillations in 1/B at 1.3 K due to magnetic breakdown in the Z-R-A plane.*

[1] C. Fang, H. Weng, Xi Dai and Z. Fang, Chin. Phys. B **25**, 117106 (2016).
[2] T.E. O'Brien, M. Diez, and C.W.J. Beenakker, Phys. Rev. Lett. **116**, 236401 (2016).
[3] M.R. van Delft *et al.*, *in preparation.*
[4] S. Pezzini *et al.*, Nature Physics **14**, 178183 (2018).

Talk-Tuesday afternoon

Topological Hall effect in different microscopic regimes

K.S. Denisov,[1,2] I.V. Rozhansky,[1,2] N.S. Averkiev,[1] and E. Lahderänta[2]

[1] *Ioffe Institute, Saint-Petersburg, Russia*

[2] *Lappeenranta University of Technology, Lappeenranta, Finland*

In this work we develop the theory of topological Hall effect (THE) in different microscopic regimes. The THE manifests itself as an additional Hall voltage in magnetic systems possesing a non-collinear ordering of magnetic moments. The microscopic origin of THE is an electron asymmetric scattering on non-collinear magnetic textures, such as magnetic skyrmions. This phenomenon has recently attracted a great interest, since it provides a new transport tool for the detection of a chiral magnetic textures in media. Whereas the family of materials where THE has been observed gradually expands, it has become evident that THE has a number of nontrivial features complicating both its theoretical and experimental treatments.

In this talk we discuss the intrinsic nontrivial behaviour of THE, which appears due to the existence of different microscopic regimes of this phenomenon [1]. We consider the case, when the Fermi energy is large and both carrier spin subbands are activated. It turns out, that THE exhibits different features depending on whether the carrier spin flip processes are activated or not. The presence of spin-flip processes is controlled by the adiabatic parameter $\lambda_a = \omega_{ex}\tau$, where $\hbar\omega_{ex}$ is an exchange interaction constant, and τ is a characteristic time of a carrier fly trough the non-collinear texture core. In our work we have developed a unified theoretical approach capable of describing THE for an arbitrary value of λ_a and covering all microscopic scenarios. Our theory is based on the exact calculation of an itinerant carrier scattering cross-section on a localized non-collinear magnetic texture, such as magnetic skyrmion. We apply this approach to calculate THE within the diffusive regime, typical for magnetic semiconductor systems.

Let us consider in details the properties of THE in different regimes with respect to λ_a. For $\lambda_a \leq 1$ the carrier exchange interaction with a single skyrmion is quick and the spin-flip processes are activated. As we demonstrated in [2], the asymmetric scattering in this regime appears due to the interference between double spin-flip scattering and single spin-conserving scattering. The hallmark of the spin-chirality driven mechanism is that the resulting sign of the scattering asymmetry appears to be the same for all scattering channels. This indicates that for $\lambda_a \leq 1$ the charge transverse response dominates over spin Hall effect and THE appears even for totally spin unpolarized carriers. In the opposite regime of large $\lambda_a \gg 1$ the adiabatic theorem states that the spin flip processes are suppressed. In this case, the scattering asymmetry is due to the geometrical Berry phase acquired by an electron motion through a non-collinear magnetization area. The hallmark of this regime is that spin up and spin down electrons are scattered in opposite transverse directions thus creating the spin Hall effect. In the adiabatic regime ($\lambda_a \gg 1$) the THE appears only due to non-zero carrier spin polarization.

The topological Hall effect resistivity ρ_H^T in the diffusive regime consists of two microscopically different contributions $\rho_H^T = \rho_H^c + \rho_H^a$, where ρ_H^c is spin-chirality driven term due to spin-flip scattering on triads of non-collinear spins [2], and ρ_H^a is the adiabatic term due to spin-dependent Berry phase. The hallmark of ρ_H^c is that it does not depend on a carrier spin polarization and its sign is determined by the orientation of non-collinear texture in its center. As ρ_H^c term is activated by spin-flip processes, it decreases at large λ_a. The adiabatic mechanism ρ_H^a is directly coupled to carrier spin polarization. Since the ρ_H^a appears after the suppression of spin flip scattering channels, there exists a crossover regime (the intermediate range of λ_a), where both ρ_H^c, ρ_H^a contributions are of the same order of magnitude. Our calculation shows that in this regime the ρ_H^T depends non-monotonically on skyrmion size and Fermi level [1].

The non-monotonic crossover between spin-chirality driven and adiabatic mechanisms is the most striking feature of THE. Nevertheless, it is still challenging to access this physics in experiments, which is mainly due to the poor tuneability of materials where THE has been observed so far. We would like to draw the attention that the 2D systems based on diluted magnetic semiconductors are highly promising for the experimental investigation of this issues. These compounds allow one to control both the Fermi energy and the magnitude of exchange interaction, which provides one an experimental access to the discussed physics of THE. The particular mechanisms of non-collinear ordering of magnetic impurities in semiconductor nanostructures are going to be discussed in more details by our group in the following conference ICPS-2018.

[1] K.S. Denisov, I.V. Rozhansky, N.S. Averkiev *et al.* Sci. Rep., **7**, 17204, (2017)

[2] K.S. Denisov, I.V. Rozhansky, N.S. Averkiev *et al.* Phys. Rev. Lett., **117**, 027202, (2016)

Strong anisotropic in-plane magneto-transport in a few-layer bP FET

Francesca Telesio,[1] Nicholas Hemsworth,[2] Will Dickerson,[2] Matei Petrescu,[3] Vahid Tayari,[2] Oulin Yu,[3] David Graf,[4] Manuel Serrano-Ruiz,[5] Maria Caporali,[5] Maurizio Peruzzini,[5] Danil Bukhvalov,[6] Thomas Szkopek,[2] Stefan Heun,[1] and Guillaume Gervais[3]

[1]*NEST, Istituto Nanoscienze–CNR and Scuola Normale Superiore, I-56127 Pisa, Italy*

[2]*Department of Electrical and Computer Engineering, McGill University, Montréal, Québec, H3A 2A7, Canada*

[3]*Department of Physics, McGill University, Montréal, Québec, H3A 2T8, Canada*

[4]*National High Magnetic Field Laboratory, Tallahassee, FL 32310, United States*

[5]*Istituto di Chimica dei Composti OrganoMetallici–CNR, I-50019 Sesto Fiorentino, Italy*

[6]*Department of Chemistry, Hanyang University, 17 Haengdang-dong, Seongdong-gu, Seoul 04763, Republic of Korea*

Since its re-discovery in 2014 as a van der Waals material suitable for mechanical exfoliation, black phosphorus (bP) has attracted great interest, mostly due to its direct band gap that depends on the number of layers, as well as its strong in-plane anisotropy. This latter property is caused by the puckered structure of the individual bP planes forming the atomic crystal, see Fig. 1(b). This anisotropy has been observed in its optical, thermal, and electronic transport properties [1,2], as well as in quantum-interference effects such as weak localization [3].

Previous magneto-transport focused mainly on the Shubnikov-de Haas oscillations [4] and on the quantum Hall effect [5]. Here, we report in-plane magneto-resistance measurements of few-layer bP forming a field-effect transistor, see Fig. 1(c). The resistivity was determined as a function of the angle between the in-plane magnetic field and the crystallographic axis of the bP flake, as determined by polarized Raman spectroscopy. The observed in-plane magnetoresistance is found to be as large as 10%, is strongly anisotropic, and it varies non-monotonically with increasing field up to 45T (at a fixed angle), shown in Fig. 1(a). The conventional theory of magneto-resistivity drastically fails to account for the behaviour observed at such large fields. In this regime, the magneto-resistance exhibits clear maxima (minima) when the magnetic field is aligned along the zig-zag (armchair) axis. Taking anisotropy into account and introducing a correction for the carriers' velocity due to the Lorentz force, a model was developed that remarkably captures the essence of this anisotropic magneto-resistive effect.

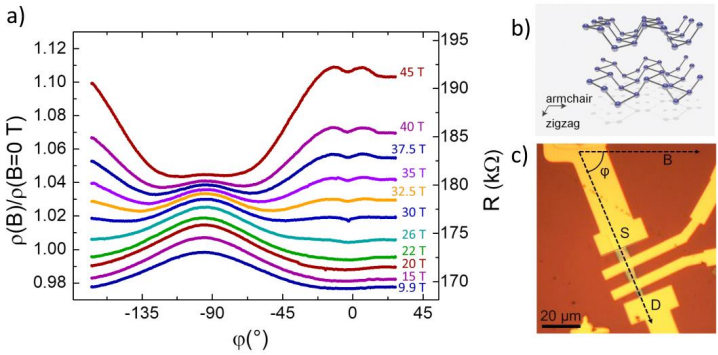

FIG. 1. (a) Low-temperature in-plane magneto-resistance as a function of azimuthal angle φ between the device axis and magnetic field vector. (b) Sketch of bP crystal structure with crystallographic directions indicated. (c) Optical microscopy image of the device with source (S) and drain (D) indicated. The angle φ is indicated.

[1] Xia, F., Wang, H. & Jia, Y. Rediscovering black phosphorus as an anisotropic layered material for optoelectronics and electronics. Nat. Commun. 5, 4458 (2014).
[2] Luo, Z. et al. Anisotropic in-plane thermal conductivity observed in few-layer black phosphorus. Nat. Commun. 6, 8572 (2015).
[3] Hemsworth, N. et al. Dephasing in strongly anisotropic black phosphorus. Phys. Rev. B 94, 245404 (2016).
[4] Tayari, V. et al. Two-Dimensional Magnetotransport in a Black Phosphorus Naked Quantum Well. Nat. Commun. 6, 7702 (2015).
[5] Li, L. et al. Quantum Hall effect in black phosphorus two-dimensional electron system. Nat. Nanotechnol. 11, 593 (2016).

The authors thank the European Research Council (ERC) under the European Union's Horizon 2020 research and innovation program (Grant Agreement No. 670173) for funding the project PHOSFUN "Phosphorene functionalization: a new platform for advanced multifunctional materials" through an ERC Advanced Grant.

High field transport properties of 2DEG at the $LaAlO_3/SrTiO_3$ interface with varying gate tunable carrier density

K. Rubi[1], M. Yang[1], B. Kerdi[1], K. Han[2], S. Zeng[2], M. Pierre[1], Ariando[2], M. Goiran[1] and W. Escoffier[1]

[1]*Laboratoire National des Champs Magnetiques Intenses (LNCMI-EMFL), CNRS-UGA-UPS-INSA, 143 Avenue de Rangueil, 31400 Toulouse, France*

[2]*Department of Physics and NUSNNI-Nanocore, National University of Singapore, Singapore 117411*

Abstract

The formation of a two-dimensional electron gas (2DEG) at the interface between two insulators $SrTiO_3$ (STO) and $LaAlO_3$ (LAO) is among the most intriguing findings in oxide electronics. While the gate tunable superconductivity [1] and spin orbit coupling [2] at this interface are well studied, no clear consensus is reached on the quantum oscillations tuned with gate voltage. We have investigated the quantum transport of a high mobility 2DEG at LAO/STO interface under high magnetic field (55T). The Shubnikov-de Haas (SdH) oscillations in longitudinal resistance (R_{xx}) show a clear monotonic dependence with varying the gate voltage/carrier density (see Fig. 1), despite a one order of magnitude discrepancy between the carrier concentrations estimated from the Hall resistance and the SdH oscillation's frequency [3]. Interestingly, the Landau fan diagram is non-linear implying the presence of many sub-bands derived from the Ti:3d orbitals (d_{xy}, d_{xz} and d_{yz}) of STO and/or sub-band spin-spitting at the Fermi energy in the band structure. The substantial shift in the amplitude and frequency of the oscillations observed with varying back-gate voltage allows investigating the complex band structure of this 2DEG.

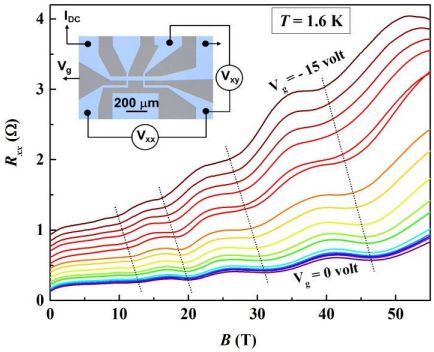

Figure 1. The magnetic field dependence of longitudinal resistance (R_{xx}) with varying back-gate voltage. The dot lines are guides for the eye. The inset shows an optical micrograph of LAO/STO device.

References

[1] A. Joshua *et. al.*, Nature Comm. **3**, 1129 (2012); J. Biscaras *et. al.*, Phys. Rev. Lett. **108**, 247004 (2012).
[2] A. D. Caviglia *et. al.*, Phys. Rev. Lett. **104**, 126803 (2010); M. Ben Shalom *et. al.*, Phys. Rev. Lett. **104**, 126802 (2010); Z. Zhong *et. al.*, Phys. Rev. B **87**, 161102(R) (2013).
[3] M. Yang *et. al.*, App. Phys. Lett. **109**, 122106 (2016).

Observation of crossover from a complex stripe phase to a helical phase in multiple one-atomic-layer films

Ryuichi Masutomi,[1] Shotaro Tashiro,[1] Tohru Okamoto,[1] and Youichi Yanase[2]

[1] *Department of Physics, University of Tokyo, Tokyo, Japan*

[2] *Department of Physics, Kyoto University, Kyoto, Japan*

The Larkin–Ovchinnikov state (generally known as the Fulde–Ferrell–Larkin–Ovchinnikov state) is a novel superconducting state in which the magnitude of the superconducting order parameter modulates in the real space due to the formation of Cooper pairs with a finite center-of-mass momentum in a strong magnetic field. It has been observed in heavy fermion superconductors and organic superconductors. However, the direct evidence of the helical state (also referred to as the Fulde–Ferrell state), which is characterized by the phase modulation of the superconducting order parameter, has not yet been observed. In this study, we report the first observation of both the helical phase and the complex stripe phase, characterized by both magnitude and phase modulations of the superconducting order parameter, in multiple one-atomic-layer Pb films with a layer-dependent strong Rashba spin-orbit interaction.

To observe these exotic superconducting states, we fabricated bilayer and trilayer films on the cleaved surface of a non-doped insulating GaAs substrate, which comprise one-atomic-layer Pb films with a strong Rashba spin-orbit interaction caused by the breaking of the space inversion symmetry, as depicted in the insets of Fig. 1. The detailed sample preparation and experimental procedure are shown in Ref. [1-3]. In these multilayer films, each of the one-atomic-layer Pb film is weakly coupled with a spacer layer of Sb, and it has a layer-dependent Rashba spin-orbit interaction due to an opposite potential gradient along the normal direction of the two-dimensional plane.

After the sample preparation, we performed *in situ* magneto-transport measurements to obtain the temperature dependence of the parallel upper critical magnetic field $B_{c2}^{\parallel}$ for the multilayer films. The data are depicted in Fig. 1. As expected in two-dimensional systems, the temperature dependence of $B_{c2}^{\parallel}$ for the bilayer film varies as a negative square-root. In contrast, for the trilayer film, a steep upturn is observed in the measurement of the temperature dependence of $B_{c2}^{\parallel}$. From the numerical calculations performed using the Bogoliubov–de Gennes equations, we find that this upturn corresponds to the crossover from the complex stripe phase to the helical phase in the multiple one-atomic-layer films. In this study, we also present the phase diagram of the multiple one-atomic layer Pb films; it was determined from both experimental observations of the crossover from the complex stripe phase to the helical phase and from the numerical results obtained by the Bogoliubov–de Gennes equations. Our findings pave the way for the elucidation of non-trivial superconducting states in multilayer systems composed of two-dimensional Rashba superconductors.

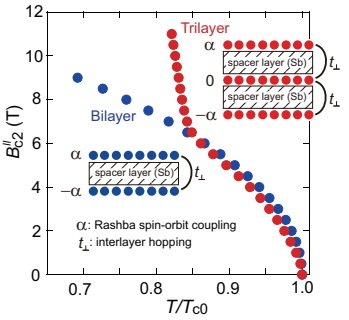

FIG. 1. *Temperature dependence of the parallel upper critical magnetic field $B_{c2}^{\parallel}$ for bilayer and trilayer films. The red (blue) closed circles denote the data for the trilayer (bilayer) film. The film thickness of the Sb spacer layer is* 2.0 nm.

[1]T. Sekihara, R. Masutomi, and T. Okamoto, Phys. Rev. Lett., **111**, 057005 (2013).

[2]R. Masutomi and T. Okamoto, Appl. Phys. Lett., **106**, 251602 (2015).

[3]M. Niwata, R. Masutomi, and T. Okamoto, Phys. Rev. Lett., **119**, 257001 (2017).

Bandstructure engineering with patterned dielectric superlattices

Carlos Forsythe,[1] Xiaodong Zhou,[1] Takashi Taniguchi,[2] Kenji Watanabe,[2] Abhay Pasupathy,[1] Pilkyung Moon,[3] Mikito Koshino,[4] Philip Kim,[5] and Cory R. Dean[1]

[1] *Department of Phyics, Columbia University, USA*

[2] *National Institute for Materials Science, Japan*

[3] *NYU Shanghai, Shanghai 200122, China*

[4] *5Department of Physics, Osaka University, Japan*

[5] *6Department of Physics, Harvard University, USA*

The ability to manipulate two-dimensional (2D) electrons with external electric fields provides a route to synthetic band engineering. By imposing artificially designed and spatially periodic superlattice (SL) potentials, 2D electronic properties can be further engineered beyond the constraints of naturally occurring atomic crystals. Here we report a new approach to fabricate high mobility SL devices by integrating surface dielectric patterning with atomically thin van der Waals materials. By separating the device assembly and SL fabrication processes, we address the intractable tradeoff between device processing and mobility degradation that constrains SL engineering in conventional systems. The improved electrostatics of atomically thin materials moreover allows smaller wavelength SL patterns than previously achieved. Replica Dirac cones in ballistic graphene devices with sub 40nm wavelength SLs are demonstrated, while under large magnetic fields we report the fractal Hofstadter spectra from SLs with designed lattice symmetries vastly different from that of the host crystal. Our results establish a robust and versatile technique for band structure engineering of graphene and related van der Waals materials with dynamic tunability.

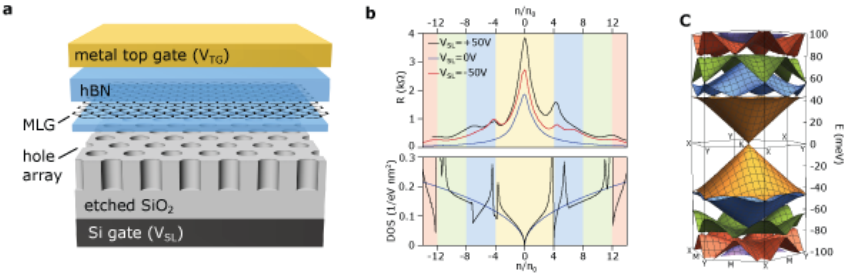

FIG. 1. *(a) Cartoon schematic of our patterned dieletric superlattice device structure. (b) Transport measurement at zero magnetic field (top panel) versus density showing excellent correspondence to the theoretically calculated density of states (bottom panel). (c) Modified graphene bandstructure calculated for the device structure shown in (a).*

[1]C. Forsythe *et al.* arXiv:1710.01365 (2018)

Effective interaction, bandgap renormalization and massive Dirac Fermion excitons in magnetic field

L. Szulakowska[1], M.Bieniek[1,2] and P. Hawrylak[1]
[1]*Department of Physics, Advanced Research Complex, University of Ottawa, Ottawa, Canada*
[2]*Department of Theoretical Physics, Wroclaw University of Science and Technology, Wroclaw, Poland*
lszul050@uottawa.ca

We present here theory describing the effect of the strong magnetic field on bandgap renormalization and exciton spectrum in a class of two-dimensional crystals, from graphene in a staggered potential to transition metal dichalcogenides (TMDCs) [1-6], which can be described by a gapped massive Dirac Fermion (mDF) model.

We start with an ab-initio based next-nearest neighbour tight-binding (TB) model [4,6] which reduces to the massive Dirac Fermion model close to K-points. We derive effective intra and inter valley screened e-e interactions and discuss the exciton spectrum at zero magnetic field[5]. We next turn on the magnetic field which leads to the formation of Landau levels[6-8] and Lande and Valley Zeeman splitting. To describe the role of electron-electron interactions in optical transitions of mDF in strong magnetic fields [9] we start from the single-particle effective Dirac Hamiltonian with spin-valley-dependent low-energy gap obtained within our TB model. We populate the N valence mDF levels and construct the Hartree-Fock (HF) ground state. We create quasi-electron and quasi-hole excitations out of the HF ground state, calculate self-energy, direct and exchange vertex corrections and solve numerically the Bethe-Salpeter equation to obtain the magneto-exciton spectrum in the two non-equivalent valleys. We discuss how intervalley exchange interaction leads to fine structure in the magnetoexciton spectrum. The absorption and emission spectra are calculated as a function of the mass-term, from massive to massless Dirac fermions, electron-electron interaction strength and magnetic field. The magneto-exciton spectra are compared with experiments [10,11].

References

[1] K. F. Mak, C. Lee, J. Hone, J. Shan, and T. F. Heinz, Phys. Rev. Lett. **105**, 136805 (2010).
[2] E. Kadantsev, and P. Hawrylak, Solid State Commun. **152**, 909 (2012).
[3] X. Xu, W. Yao, D. Xiao, and T. F. Heinz, Nature Phys. **10**, 343–350 (2014).
[4] T. Scrace, Y. Tsai, B. Barman, L. Schweidenback, A. Petrou, G. Kioseoglou, I. Ozfidan, M. Korkusinski, and P. Hawrylak, Nature Nanotechnology **10**, 603–607 (2015).
[5] Diana Y. Qiu, Ting Cao and Steven G. , Phys.Rev.Lett. 115, 176801 (2015).
[6] M. Bieniek, M. Korkusinski, L. Szulakowska, P. Potasz, I. Ozfidan, P Hawrylak, Phys.Rev.B 97, 085153 (2018)..
[7] F. Rose, M. O. Goerbig, and F. Piechon, Phys. Rev. B **88**, 125438 (2013).
[8] T. Cai, S. A. Yang, X. Li, F. Zhang, J. Shi, W. Yao, and Q. Niu, Phys. Rev. B **88**, 115140 (2013).
[9] P. Hawrylak, and M. Potemski, Phys. Rev. B **56**, 12386 (1997).
[10] A. V. Stier, K. McCreary, B. T. Jonker, J. Kono and S. A. Crooker, Nature Comm. **7**, 10643 (2016). [11] A. V. Stier, N. P. Wilson, K. A. Velizhanin, J. Kono, X. Xu, and S. A. Crooker, Phys. Rev. Lett.120, 057405 (2018).

Fine structure of dark exciton in WSe_2 monolayers in perpendicular magnetic field

Cedric Robert,[1] Emmanuel Courtade,[1] Marco Manca,[1] Bo Han,[1] Shivangi Shree,[1] Fabian Cadiz,[1] Delphine Lagarde,[1] Thierry Amand,[1] Bernhard Urbaszek,[1] and Xavier Marie[1]

[1] *Université de Toulouse, INSA-CNRS-UPS, LPCNO, 135 Avenue de Rangueil, 31077, Toulouse, France*

Transition Metal Dichalcogenides (TMDC) monolayers have emerged as exciting 2D materials as they present strong light-matter interaction governed by robust excitons and interesting spin/valley selective optical selections rules. Despite being opticall inactive, dark excitons are known to play a strong role in the optical properties of TMDC monolayers.

The splitting between bright (spin allowed) and dark (spin forbidden) excitons has been measured in tungsten-based monolayers exploiting the optical selection rules associated to in-plane propagation of light [1] or by mixing bright and dark excitons under high transverse magnetic fields [2]. The exact amplitude of this bright-dark splitting Δ depends on both conduction band spin-orbit splitting and short-range Coulomb interaction.

In this work, we will show that the short-range exchange interaction also lifts the double degeneracy of spin forbidden excitons giving rise to a perfectly dark lower energy state (electric dipole forbidden) and a higher energy state that can couple to light whith an out-of-plane polarization mode (gray exciton). We will present magnetophotoluminescence measurements in a magnetic field B_z applied perpendicular to a WSe_2 monolayer mixing dark and gray excitons. Thanks to the narrow linewidth of the transitions obtained in hBN encapsulated WSe_2 monolayers, we can extract the zero-field splitting $\delta = 0.6$ meV between dark and gray excitons [3].

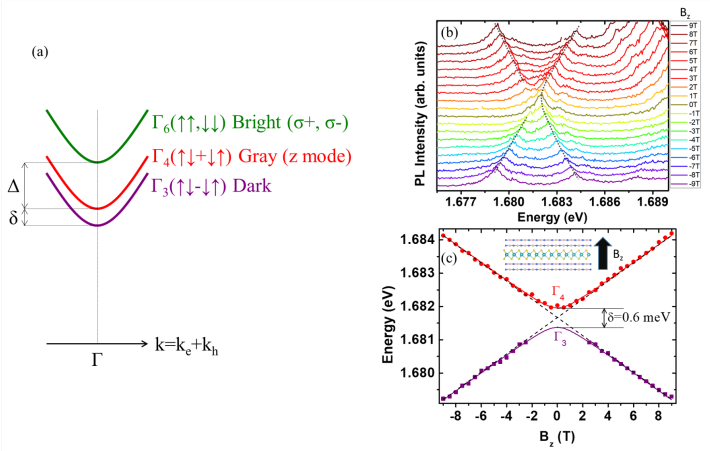

FIG. 1. *(a) Excitonic band structure of monolayer WSe_2. Bright excitons (Γ_6 states in the D_{3h} point symmetry group) are spin allowed with an electric dipole oscillating in the monolayer plane. The gray exciton Γ_4 state is spin forbidden but the electric dipole is allowed in the z mode (perpendicular to the monolayer plane) whereas the Γ_3 state is spin forbidden and electric dipole forbidden (truly dark state). (b) PL of gray and dark excitons as a function of longitudinal (perpendicular to the monolayer plane) magnetic field B_z at 4 K. Gray dashed lines are guides to the eyes pointing the energy of the transitions. At $B_z = 0T$ only the gray exciton line is observed;(c) Energy of gray and dark excitons as a function of B_z extracted from (b).*

[1] G. Wang *et al.* Phys. Rev. Lett., **119**, 047401, (2017), Y. Zhou *et al.* Nat. Nano., **12**, 856, (2017)

[2] X.-X. Zhang *et al.* Nat. Nano., **12**, 883, (2017), M. Molas *et al.* 2D Mater., **4**, 021003, (2017)

[3] C. Robert *et al.* Phys. Rev. B, **96**, 155423, (2017)

Magneto-photoluminescene spectroscopy of excited exciton states in h-BN encapsulated monolayer WSe_2 and MoS_2

M. R. Molas,[1, 2] K. Nogajewski, [1, 2] C. Faugeras,[1] Artur O. Slobodeniuk,[1] M. Bartos,[1] Ł. Bala,[1, 2] K. Watanabe,[3] T. Taniguchi,[3] A. Babiński,[2] and M. Potemski,[1, 2]

[1]*Laboratoire National des Champs Magnetiques Intenses, CNRS-UGA-UPS-INSA-EMFL, Grenoble, France*

[2]*Institute of Experimental Physics, Faculty of Physics, University of Warsaw, Warszawa, Poland*

[3]*National Institute for Materials Science, Tsukuba, Japan*

Owing to the advancement of fabrication techniques, high-quality van der Waals heterostructures consisting of different monolayer transition metal dichalcogenides (TMDs) encapsulated in hexagonal boron nitride (h-BN) have recently become an intensively exploited platform for studying nonhydrogenic interactions between electrons and holes in two-dimensional systems with dielectric confinement and nonlocal screening. In one of the latest works [1], a clear deviation of the effective Coulomb potential from the 1/r form has been demonstrated based on magnetoabsorption spectroscopy of exciton Rydberg states (up to 4*s*) in monolayer WSe_2.

In this communication we report on low-temperature helicity-resolved magneto-photoluminescence investigations of excited states of the optically active band-edge A-exciton in h-BN encapsulated monolayer WSe_2 and MoS_2. For WSe_2 we show that emission of light from up to 5*s* state can be observed at moderate magnetic fields up to 14 T. Under similar conditions, only the 1*s* and 2*s* states of the A-exciton remain visible in the photoluminescence spectra of our MoS_2 samples. In both cases, however, the zero-field 1*s* and 2*s* emission persist up to room temperature, as evidenced by independent measurements performed in a wide temperature range from 5 K to 300 K.

Based on magnetic-field evolution of the emission peaks observed (see Figure), we precisely determine the A-exciton spectrum at zero magnetic field. With the aid of respective diamagnetic shifts we also estimate the extensions of wave functions associated with the 1*s*-4*s* states in WSe_2 and 1*s*-2*s* states in MoS2. Relying on this data, the apparent shape of the effective Coulomb potential in our highly polarizable 2D systems surrounded by less polarizable medium is then examined within the framework of the so-called Keldysh approximation. A simplified analytical model to account for the energy and wavefunction's extension of the A-exciton's states in h-BN encapsulated monolayer TMDs is also proposed.

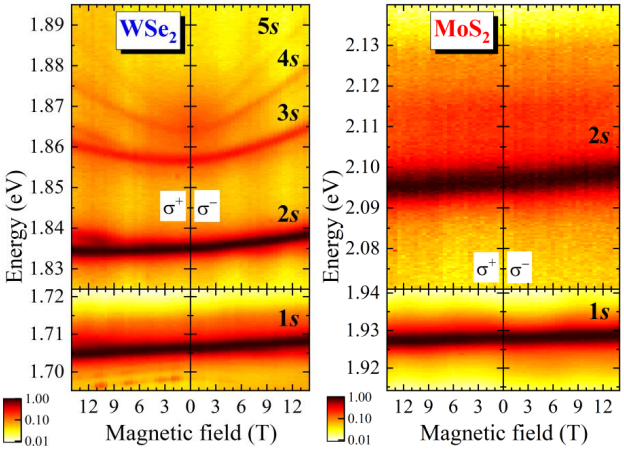

Figure: False-colour map of helicity-resolved ($\sigma^{\pm}$) low-temperature (5 K) photoluminescence spectra measured on h-BN ecapsulated monolayer WSe_2 and MoS_2 as a function of magnetic field.

[1] A. V. Stier *et al.*, Phys. Rev. Lett. **120**, 057405 (2018).

Unraveling interlayer excitons in a bulk two-dimensional semiconductor under high magnetic fields

Ashish Arora,[1] Matthias Drüppel,[2] Robert Schmidt,[1] Thorsten Deilmann,[2,3] Robert Schneider,[1] Maciej R. Molas,[4] Philipp Marauhn,[2] Steffen Michaelis de Vasconcellos,[1] Marek Potemski,[4] Michael Rohlfing,[2] and Rudolf Bratschitsch[1]

[1]*Institute of Physics and Center for Nanotechnology, University of Münster, Wilhelm-Klemm-Straße 10, 48149 Münster, Germany*

[2]*Institute of Solid State Theory, University of Münster, Wilhelm-Klemm-Straße 10, 48149 Münster, Germany*

[3]*Center for Atomic-Scale Materials Design (CAMD), Department of Physics, Technical University of Denmark, DK-2800 Kongens Lyngby, Denmark*

[4]*Laboratoire National des Champs Magnétiques Intenses, CNRS-UGA-UPS-INSA-EMFL, 25 rue des Martyrs, 38042 Grenoble, France*

High magnetic fields are instrumental in exploring fundamental physics in semiconductors and are recently being used to study semiconducting two dimensional (2D) materials.
In this presentation, I will discuss our recent discovery of Coulomb bound electrons and holes with spatially displaced wave functions called 'interlayer excitons' in bulklike $MoTe_2$ [1]. We use high-field magneto-reflectance spectroscopy with up to 29 T combined with *GW*-BSE *ab initio* calculations to unravel their existence. The constituent electrons and holes for these quasiparticle states are individually localized in the neighboring layers of the van der Waals crystal (a). These excitons are formed due to the specific spin-valley coupling of the charge carriers within the individual layers of the crystal. Interlayer excitons have an opposite sign of their g-factors and significantly larger diamagnetic shifts when compared to intralayer excitons (electron and hole in the same layer, b). I will also discuss our finding that the 2D materials preserve many salient features of the monolayer and the bilayer physics even in their bulklike form.

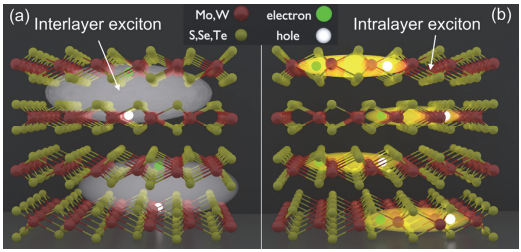

Interlayer excitons are important for Bose-Einstein condensation, superfluidity, dissipationless current flow, and the light-induced exciton spin Hall effect. Our discovery solves the long-standing puzzle of positive g-factors in van der Waals semiconductors, and paves the way for studying collective phenomena in these materials at elevated temperatures [2].

[1] A. Arora et al. Nat. Commun., 8, 639, (2017)
[2] M. M. Fogler et al., Nat. Commun. 5, 4555, (2014)

Valley polarization dynamics of interlayer excitons in 2D crystal heterostructures in high magnetic fields

Johannes Holler,[1] Jonas Zipfel,[1] Mariana V. Ballottin,[2] Anatolie A. Mitioglu,[2] Michael Kempf,[1] Philipp Nagler,[1] Fabian Mooshammer,[1] Nicola Paradiso,[1] Christoph Strunk,[1] Rupert Huber,[1] Alexey Chernikov,[1] Peter C. M. Christianen,[2] Christian Schüller,[1] and Tobias Korn[1]

[1] *Institut für Experimentelle und Angewandte Physik, Universität Regensburg, Germany*

[2] *High Field Magnet Laboratory (HFML EMFL), Radboud University Nijmegen, Netherlands*

In recent years, research in the field of two-dimensional materials has been growing fast, and since the discovery of a direct bandgap in monolayer transition-metal dichalcogenides (TMDCs), these materials became especially interesting. In addition to exciting new physical properties in individual monolayers, like spin-valley coupling, different TMDCs can be combined into heterostructures, revealing new excitonic properties.

Here, we study $MoSe_2$-WSe_2 heterostructures with a staggered band alignment. Due to this modulation, optically excited electron-hole pairs are spatially separated: the holes relax into the valence band of WSe_2 and the electrons into the conduction band of $MoSe_2$, forming interlayer excitons (IEXs). Because of this spatial separation the IEXs exhibit very long photoluminescence (PL) lifetimes in contrast to intralayer excitons. Low-temperature PL measurements in magnetic fields show a giant valley-selective splitting of the IEX luminescence, with an effective g factor of about -15, far above the values for intralayer excitons in TMDC monolayers. This splitting also leads to a near-unity valley polarization of the IEXs in sufficiently large magnetic fields [1].

Furthermore, we probe the valley dynamics of the IEX in dependence of the magnetic field. We are able to observe a slow build-up of the valley polarization after unpolarized excitation, revealing different dynamics and lifetimes for the different valleys.

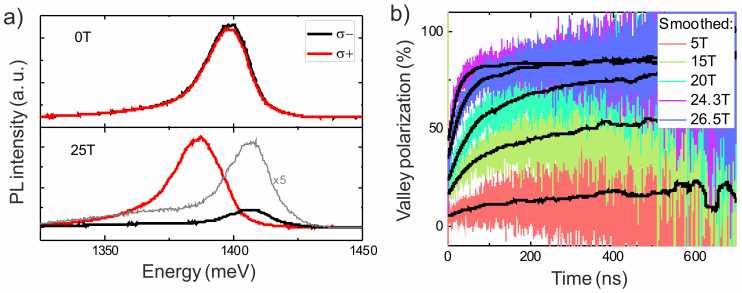

FIG. 1. *(a) Helicity-resolved PL spectra of IEX at 0 and 25 Tesla measured using linearly polarized excitation. (b) Time-dependent build-up of the valley polarization measured using linearly polarized excitation.*

[1] P. Nagler *et al.* Nat. Commun. **8**, 1551 (2017)

Magneto-optical investigation of strained 2D WSe_2 monolayers

A. Mitioglu[1,2], J. Buhot[1], M. Ballottin[1], S. Anghel[2], L. Kulyuk[2], P. C. M. Christianen[1]

[1]*High Field Magnet Laboratory (HFML - EMFL), Radboud University, NIJMEGEN, The Netherlands*
[2]*Institute of Applied Physics, Academiei Str. 5, Chisinau, MD-2028, Republic of Moldova*

Monolayer transition metal dichalcogenides (TMDCs), such as MoS_2, $MoSe_2$, WS_2 and WSe_2, are novel two dimensional materials with a direct bandgap located at two degenerate valleys (K+ and K-) at the corners of the hexagonal Brillouin zone. The energy bandgap lies in the visible spectral range, which gives rise to efficient light emission and absorption. The optical spectra in monolayer TMDCs are dominated by excitonic effects due to strong 2D confinement and electron-hole (e-h) exchange [1]. Strong spin-orbit interaction and optical selection rules enable the creation of excitons in a specific valley using circularly polarized light. In addition, linearly polarized illumination leads to excitons, whose states are a superposition of those of K+ and K- valleys, which also emit linearly polarized light due to valley coherence.
The micro-photoluminescence (PL) spectra of TMDCs are dominated by sharp neutral and charged exciton (trions) lines. Recently, we reported that under an applied magnetic field both exciton and trion emission lines of WSe_2 shift in position with magnetic field and split up into two lines of opposite circular polarization (Valley splitting). This behaviour was explained using a single-electron picture and a massive Dirac model [2]. As a result, we found an effective valley *g*-factor of 4 and a Fermi velocity of 0.51×10^6 cm^2/s. However, also significantly different g-factor values have been reported [3]. Possible origins for the spread in *g*-factors are the effects of doping or strain, although Li and co-workers [4] claimed that doping does not influence the effective g-factor. Recent theoretical work confirmed that moderate strain together with e-h exchange leads to a splitting of the exciton peak [5].

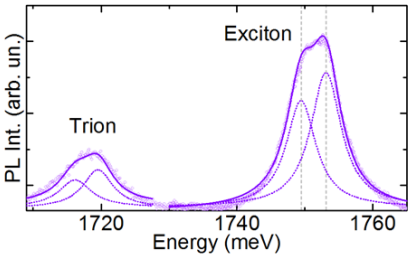

FIG. 1. Typical high resolution micro-PL spectrum of monolayer WSe_2.

High resolution micro-PL reveals that some WSe_2 flakes exhibit a PL spectrum with a splitted exciton peak (see Fig. 1). The splitting is due to a moderate intrinsic strain, as evidenced by concomitant Raman measurements. We have performed detailed polarized-resolved PL measurements on a set of strained WSe_2 flakes, in magnetic fields up to 30 T. Our results elucidate the influence of the combined effect of strain and e-h exchange on the exciton energy structure and the resulting effective *g*-factors.

[1] For a review see *e.g.* (a) X. Xu, W. Yao, D. Xiao, T. F. Heinz, *Nature Phys.* **10(5)**, 343 (2014); (b) K. F. Mak and J. Shan, *Nature Photonics* **10**, 216 (2016); (c) J. R. Schaibley, H. Yu, G. Clark, P. Rivera, J. S. Ross, K. L. Seyler, W. Yao, and X. Xu, *Nat. Rev. Mat.* **1**, 16055 (2016).
[2] A. Mitioglu, P. Plochocka, Á. Granados del Aguila, P. C. M. Christianen, G. Deligeorgis, S. Anghel, L. Kulyuk, and D. K. Maude, *Nano Lett.* **15**, 4387 (2015)
[3] G. Aivazian, Z. Gong, A. M. Jones, R-L Chu, J. Yan, D. G. Mandrus, C. Zhang, D. Cobden, W. Yao, and X. Xu, *Nature Phys.* **11**, 148 (2015)
[4] Y. Li, J. Ludwig, T. Low, A. Chernikov, X. Cui, G. Arefe, Y. D. Kim, A. M. van der Zande, A. Rigosi, H. M. Hill, S. H. Kim, J. Hone, Z. Li, D. Smirnov, and T. F. Heinz, *Phys. Rev. Lett.* **113,** 266804 (2014)
[5] (a) H. Yu et al., *Nat. Comm.* **5**, 3876 (2014); (b) H. Yu, et al., *National Sci. Rev.*, **2**, 57 (2015).

Intra- and interlayer optical transitions at $K^{\pm}$ points of transition metal dichalcogenide multilayers

A. Slobodeniuk,[1] L. Bala,[2] C. Faugeras,[1] M. Molas,[1,2] K. Nogajewski,[1,2]
M. Bartos,[1] K. Watanabe,[3] T. Taniguchi,[3] and M. Potemski[1]

[1] *Laboratoire National des Champs Magnétiques Intenses, CNRS-UGA-UPS-INSA, Grenoble, France*

[2] *Institute of Experimental Physics, Faculty of Physics, University of Warsaw, Warszawa, Poland*

[3] *National Institute for Materials Science, Tsukuba, Japan*

Intensive efforts have been recently focused on uncovering the optical properties of monolayers of semiconducting transition metal dichalcogenides (S-TMDs), whereas less attention has been paid so far on their multilayer structures.

Here we report on theoretical studies of absorption and magneto-absorption transitions which occur in the vicinity of $K^{\pm}$ points of the Brillouin zone in few-layer 2H-stacked S-TMDs. The developed model is applied to interpret the experimental data of reflectance and magneto-reflectance measurements, performed on single-, bi- and trilayers of MoS_2.

The description of optical transitions at $K^{\pm}$ points of S-TMD multilayers is carried out using the effective Hamiltonians derived as an extension of the 7-band $\mathbf{k}\cdot\mathbf{p}$ model [1,2]. The Hamiltonians are considered up to quadratic in momentum $\mathbf{k}$ terms to incorporate the magnetic field effects in S-TMDs [3,4]. We focus on the bi- and trilayers as the simplest representatives of even- and odd-layered systems. The classification of their bands and eigenstates in $K^{\pm}$ points is done with respect to the crystals' symmetry (bilayer possesses an in-plane mirror symmetry σ_h, while trilayer has an inverse symmetry i). It allows to define the two types of optical transitions in TMDC — intra- and interlayer ones, and obtain the optical selection rules for both cases.

Intra- an inter-layer transitions are demonstrated to exhibit the opposite in sign Zeeman effect. With theoretical simulations we fairly reproduce the main characteristic features of the measured reflectance and magneto-reflectance spectra and extract the model parameters of few-layer MoS_2. In particular the expected characteristic of g-factors, opposite in sign for intra and inter layer transitions, are confirmed in (polarization resolved) experiments performed in high magnetic fields. Difference in the absolute values of these g-factors is used to derive the amplitude of the so-called Zeeman valley term.

[1] A. Kormányos *et al.*, 2D Mater. **2**, 022001 (2015)

[2] G.-B. Liu *et al.*, Chem. Soc. Rev. **44**, 2643 (2015)

[3] M. R. Molas *et al.*, Nanoscale **9**, 13128 (2017).

[4] Z. Gong *et al.*, Nat. Commun. **4**, 2053 (2013).

On the quantum limit of a single Fermi surface pocket - $CoSb_3$ at high magnetic fields

Marcel Naumann,[1,2] Frank Arnold,[1] Tobias Förster,[3] Helge Rosner,[1]
Mirtha Pillaca Quispe,[4] Peter Gille,[4] and Elena Hassinger[1,2]

[1] *Max-Planck-Institut für Chemische Physik fester Stoffe, 01187 Dresden, Germany*

[2] *Physik-Departement, Technische Universität München, 85748 Garching, Germany*

[3] *Hochfeld-Magnetlabor Dresden (HLD-EMFL), Helmholtz-Zentrum Dresden-Rossendorf, 01328 Dresden, Germany*

[4] *Ludwig-Maximillians-Universität München, 80333 München, Germany*

Applying a magnetic field large enough to confine a three-dimensional electron gas into its lowest Landau level (i. e. the 'quantum limit') can induce a wide variety of quantum many-body effects, such as charge- and spin-density waves or the integer and fractional quantum Hall effects [1].

Much work has been done regarding these effects in multiband semimetals (e.g. bismuth, graphite or the TaAs-family of monopnictides). Since the theoretical description of their quantum limit physics proves to be non-trivial, systems with simpler electronic structures are of high interest. Slightly doped semiconductors, hosting a single isotropic Fermi surface, are hence promising candidates. Here, however, a magnetic field induced metal insulator transition due to the presence of an impurity band is often reported [2].

In this work, we show magnetotransport results from high quality single crystals of $CoSb_3$, a naturally lightly p-doped semiconductor. The charge carrier concentration of $n = 5 \cdot 10^{17}\mathrm{cm}^{-3}$ results in a quantum limit as low as 20 T, rendering it suitable for study of the aforementioned physics at state of the art pulsed field facilities.

In temperatures down to 1.3 K and fields up to 70 T both the resistivity perpendicular to the magnetic field ρ_{xx} and the resistivity along the field direction ρ_{zz} strongly increase for fields above the quantum limit (see figure 1). At the same time, the Hall coefficient starts to reduce at low temperatures and high fields. All these findings are in strong analogy to n-doped InSb and point to a magnetic field induced localisation of the electrons in $CoSb_3$.

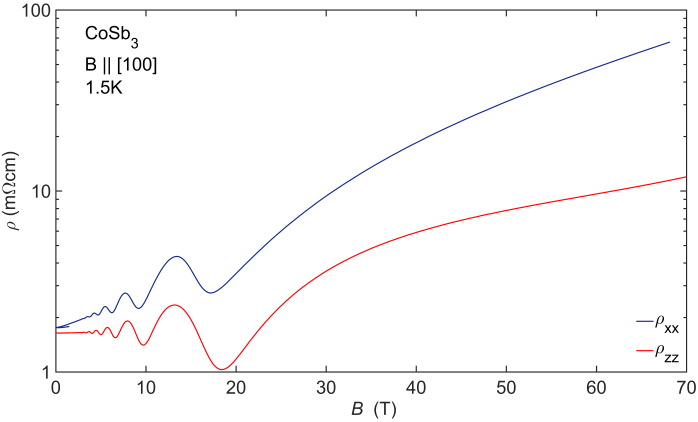

FIG. 1. *The magnetic field dependence of the transverse resistivity $I \perp B$ ρ_{xx} (dark blue) and the longitudinal resistivity $I \parallel B$ ρ_{zz} (red) at 1.5 K.*

[1] Halperin Jpn. Appl. Phys. **26**, 1913 (1987)

[2] Shayegan *et al.* Phys. Rev. B, **38**, 5585, (1989)

Quantum limit thermopower in the metallic semiconductor InSb

M. Shahrokhvand, T.W. Maas, S. Pezzini, S. Wiedmann, and U. Zeitler

High Field Magnet Laboratory (HFML-EMFL) and Institute for Molecules and Materials, Radboud University, 6525 ED Nijmegen, The Netherlands

Thermopower (TEP) is a sensitive tool to probe electronic properties of newly emerging materials. For example, recently, the interest on three-dimensional materials with high carrier mobility such as Bi [1], BiSb [2] and graphite [3] has been renewed and a giant spin Seebeck effect has been found in InSb with Pt contact stripes [4]. For a fundamental understanding of these effects a simple model system can be very helpful and therefore we investigate the high-field TEP of metallically-doped InSb, a three-dimensional semiconductor with a conceptually simple band structure, a low effective electron mass and a high mobility.

We have measured the TEP of InSb single crystals with two different carrier concentrations; $n = 2.4\times10^{17}$cm^{-3} (S1) and $n = 2.8\times10^{16}$ cm^{-3} (S2). With these concentrations we are able to access both the quantum oscillations regime as well as the extreme quantum limit where a magnetic-field induced Mott-Anderson transition is predicted [5].

In S1, we observe quantum oscillations in both S_{xx} and S_{xy}, (Fig. 1a). Interestingly, the oscillation amplitudes in S_{xx} are more pronounced compared to S_{xy}. This can be attributed to the fact that S_{xx} is governed by both phonon drag and diffusion whereas S_{xy} is only sensitive to diffusion; indeed, such a behaviour has also been observed in metallically doped HgSe [6]. In addition, spin splitting in S_{xx}, is clearly resolved whereas it is merely visible in resistance, indicating that TEP is less sensitive to scattering and therefore able to probe less pronounced energy splitting in the electronic spectrum.

In S2 we distinguish two different regimes; quantum oscillations (I) and metal-insulator transition (II), visible in both TEP (Fig. 1b) and resistance R_{xx} (Fig. 1c). This observation will allow us to quantitatively access the nature of the metal-insulator transition from two complementary experimental perspectives.

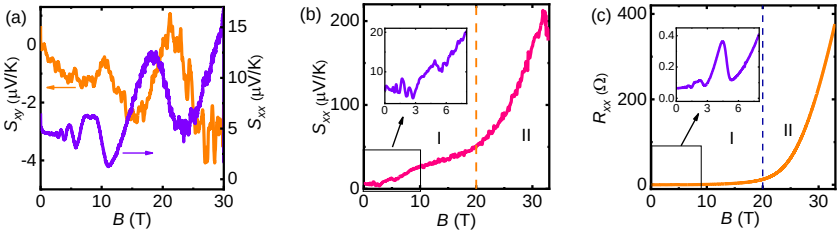

Figure 1:
(a) S_{xx} (right axis) and S_{xy} (left axis) for S1 in the quantum oscillation regime at T=18.9 K.
(b) S_{xx} for S2 at T=1.9 K showing quantum oscillations (regime I) and a metal-insulator transition (regime II).
(c) R_{xx} for S2 at T=1.3 K in the same field range as in (b).

[1] K. Behnia, M-A. Measson, and Y. Kopelevich, Phys. Rev. Lett **98**, 166602 (2007).
[2] A. Banerjee *et al.*, Phys, Rev. B **78**, 161103(R) (2008).
[3] B. Fauqué *et al.*, Phys. Rev. Lett. **106**, 246405 (2011).
[4] C. M. Jaworski *et al.*, Nature **487**, 210 (2012).
[5] S Ishida, JPSJ **72**, 151 (2003).
[6] B. Tieke *et al.*, Phys, Rev. B **54**, 15 (1996).

High-speed bolometry from Johnson noise detection of hot electrons in cavity-coupled graphene

D. K. Efetov, A. Ali, X. Lu, K. J. Tielrooij, C. Tan, Y. Gao, R.-J. Shiue, E. Walsh, F. H. L. Koppens, J. Hone, K. C. Fong, D. Englund

ICFO, Barcelona, Spain, Columbia University, New York, USA; MIT, Cambridge, USA
Dmitri.efetov@icfo.eu

High sensitivity and fast response are the most important metrics for infrared sensing and imaging and together form the primary tradeoff space in bolometry. To simultaneously improve both characteristics requires a paradigm shift on the thermal properties of bolometric materials. Due to a vanishingly small density of states at the charge neutrality point, graphene has a record-low electronic heat capacity which can reach values approaching one Boltzmann constant Ce ~ kb. In addition, its small Fermi surface and the high energy of its phonons result in an extremely weak electron-phonon heat exchange. The combination will allow a strong thermal isolation of the electrons in graphene for higher sensitivity without sacrificing the detector response time. These unique thermal properties and its broadband photon absorption, make graphene a promising platform for ultrasensitive and ultra-fast hot electron bolometers, calorimeters and single photon detectors for low energy light.

Here, we introduce a hot-electron bolometer based on a novel Johnson noise readout of the electron gas in graphene [1,2,3], which is critically coupled to incident radiation through a photonic nanocavity. This proof-of-concept operates in the telecom spectrum, achieves an enhanced bolometric response at charge neutrality with a noise equivalent power NEP < 5pW/√Hz, a thermal relaxation time of τ < 34ps, an improved light absorption by a factor ~3, and an operation temperature up to T=300K [3]. Altogether this shows that our proof-of-concept device can be a promising bolometer with efficient light absorption and a superior sensitivity-bandwidth product. Since the detector also has no limitations on its operation temperature, it provides engineering flexibility, which overall opens a new route for practical applications in the fields of thermal imaging, observational astronomy, quantum information and quantum sensing. In particular, since it is more than 5 times faster than the bandwidth of the intermediate frequency in the hot electron bolometer mixer, it can be employed as a cutting edge bolometric mixer material.

References

[1] K. C. Fong, PRX, 2 (2012);
[2] J. Crossno et.al., Science, 351 (2016);
[3] D. K. Efetov et. al., (accepted to Nature Nano. (2018));

Figures

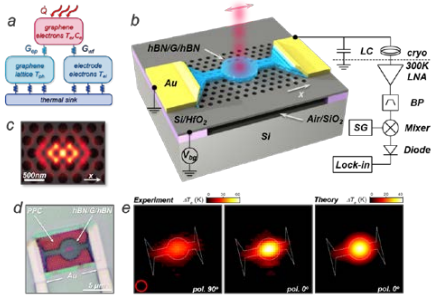

Figure 1: Figure 1: Device schematics and operation principle. (a) Schematics of heat dissipation channels of irradiated hot electrons in graphene. (b) Schematic of the device, which consists of a side contacted hBN/G/hBN heterostructure on top of a suspended silicon L3 PPC. The device is impedance matched to a LC network at cryogenic temperatures and is read out by a heterodyne JNR thermometry scheme at room temperature. (c) Resonant modes form in the L3 PPC. (d) Optical microscope image of the device. (e) Map of the bolometric response of the device as a function of laser position (red circle – laser spot size). Overall the bolometric response occurs only when the laser beam is injected on the graphene covered area, which is strongly enhanced when the PPC mode is on resonance.

Ballistic electrons splashing down in a Fermi sea

R. H. Rodriguez[1], F. D. Parmentier[1], P. Roulleau[1], U. Gennser[2], A. Cavanna[2], F. Portier[1], D. Mailly[2], & P. Roche[1]

[1]SPEC, CEA, CNRS, Université Paris-Saclay, CEA-Saclay 91191 Gif-sur-Yvette, France.
[2]CNRS, C2N, Phynano team, route de Nozay, 91460 Marcoussis, France.

The one-dimensional, chiral and dissipationless edge channels of the quantum Hall effect form the electrical analogue of fiber optics, allowing the implementation of electron quantum optics experiments where one coherently manipulates the trajectories of single electronic wave packets [1]. A recent series of experimental and theoretical works have put into light strong effects of decoherence and energy relaxation caused by interactions with quasiparticles present in neighboring edge channels, capacitively coupled to the edge channel in which the experiment is performed [2,3]. This coupling leads to new eigenstates of transport in quantum Hall edge channels, challenging the usual representation of transport in the quantum Hall effect in terms of fully independent edge channels.

We have experimentally investigated the energy relaxation undergone by a steady stream of electrons emitted at a well-defined energy in a quantum Hall edge channel, in presence of a second edge channel copropagating along the former. Our setup relies on a pair of electrostatically defined quantum dots, used as energy-resolved emitter and detector. The emitter is realized by applying a finite drain-source voltage on the first quantum dot, with a single resonant level in the bias window, the position of which sets the energy at which electrons are emitted above the drain Fermi energy. After a tunable propagation length in the micrometer scale, we perform an energy spectroscopy of the emitted electrons using the second quantum dot as an energy filter [4]. This detection technique was previously used to characterize the energy relaxation for an out-of-equilibrium energy distribution of electrons generated in a quantum point contact [5].

Our results, obtained at filling factor 2 of the quantum Hall effect, show that although the propagation over submicron lengths leads to sizable energy relaxation, a small portion of quasiparticles are not affected by energy relaxation even at relatively high energies, up to 150 µeV. Surprisingly, we observe that the amount of energy lost during propagation is markedly larger than expected [6], suggesting that relaxation mechanisms towards external degrees of freedom play an important, unexpected role in electron quantum optics experiments.

[1] E. Bocquillon, *et al.,* Annalen der Physik 526, 1 (2014).
[2] I. Levkivskyi, *et al.,* PRB 85, 075309 (2012).
[3] E. Bocquillon, *et al.,* Nat. Commun. 4, 1839 (2013).
[4] C. Altimiras, *et al.,* Nature Physics 6, 34 (2009).
[5] H. le Sueur, *et al.,* PRL 105, 056803 (2010).
[6] C. Grenier et al, Mod. Phys. Lett. B 25, 1053 (2011).

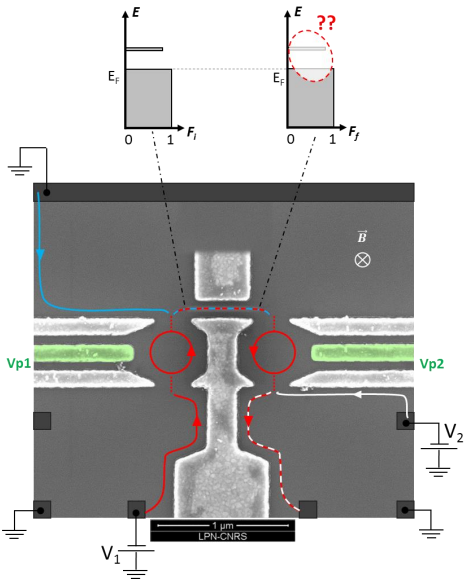

SEM view of a typical device, with the trajectories of the outer edge channel shown as red, blue and white arrows. The left quantum dot is used to inject quasiparticles at a finite energy above the Fermi level, and the right quantum dot performs their spectroscopy after propagation. The two cartoons on top schematize the energy distribution of the particles after emission and propagation.

Transport of optically pumped spin in magnetized 2D electron system

A. V. Gorbunov,[1] V. A. Kuznetsov,[1,2] A. S. Zhuravlev,[1] L. V. Kulik,[1] V. B. Timofeev,[1] I. V. Kukushkin[1]

[1]*Institute of Solid State Physics, Russian Academy of Sciences, Chernogolovka, Moscow region, 142432 Russia*

[2]*National Research University Higher School of Economics, Moscow, 101000 Russia*

The problem of dissipationless spin transport in solids occupies minds since the middle of the last century but is yet to be solved. Non-dissipative spin transport had been theoretically predicted for some materials like ferromagnetic insulators with easy-plane magnetic anisotropy or zeroth Quantum Hall state of graphene. In the discussed materials, the spin carriers may be not only electrons but also the collective excitations of the electron system, the magnons, and even so exotic topological magnetic excitations as skyrmions. However, most experimental efforts showed spin diffusion length in a very limited range [1].

Here we report on spin propagation length in the millimeter range. The spins are created by optical pumping a two-dimensional (2D) electron system in the Hall insulator state (filling factor $\nu = 2$). In a Hall insulator, the electron Fermi level lies in the cyclotron gap separating the electron states of the zeroth and first electron Landau levels. The lowest energy spin excitations are the cyclotron spin-flip excitons (CSFEs) composed of an excited electron with flipped spin in the first electron Landau level and an effective Fermi hole in the zeroth electron Landau level. These excitations are electrically neutral quasiparticles with total spin $S = 1$, which obey the Bose-Einstein statistics. In the case of CSFEs electron-hole symmetry is exhibited, wherein the mass and charge of the excited electron are equal to those of the effective Fermi hole. The CSFEs have a remarkable dispersion law [2] allowing them to move dissipationless in the absence of the random potential. The propagation of CSFEs is related to neither the charge transfer nor the mass transfer, but to the transfer of energy and spin. Very important is that CSFEs are spin-triplet excitons. Their radiative relaxation is forbidden in dipole approximation, i.e. CSFEs are optically "dark". The spin presence in a macroscopic area surrounding photoexcitation spot can be visualized with an original optical technique of spatially resolved photo-induced resonant reflection [3]. The object of our study was a high-quality GaAs/AlGaAs heterostructure with a 35-nm-wide symmetrically doped single GaAs quantum well. The electron concentration in the 2D channel was 2×10^{11} cm^{-2} at the dark mobility exceeding 15×10^{6} cm^2/V·s. At temperatures below 1 K, the lifetime of CSFEs in our samples reached unprecedented millisecond range [4]. Therefore, in experiments a high-density spin exciton gas could be created avoiding system overheating [4].

In the quantizing magnetic field the theoretically estimated mean free path for the single spin excitation in the volume of the Hall insulator is below 1μm. We observe, indeed, that at low CSFEs concentration when the spin-triplet excitons remain in the gaseous phase, the spin diffusion length does not exceed few micrometers (spatial resolution of our experimental setup), which is in good agreement with the results obtained for other electron systems. As soon as the CSFEs density reaches a critical value, a phase transition to a new condensed state, the *magnetofermionic* condensate, is observed [4]. Its formation is accompanied by an increase in spin propagation length by at least three orders of magnitude. The maximum propagation length measured in our experiments reached 2 mm and was limited by the size of the studied sample only [4]. The spin distribution from the edge of the photoexcitation spot toward the edge of the propagation spot is not described by a Gaussian distribution. Instead, a spin-density plateau is observed over the entire propagation spot. Thus, exciton transfer is not a diffusive process. Taking into account the giant propagation lengths of the spin excitations, the non-diffusive nature of the spin distribution in space, and the unique dispersion of CSFEs it is very probable that the spin propagation in a magnetofermionic condensate is non-dissipative. The spin propagation length varies with temperature. It is possible therefore to either block the spin propagation completely or permit spin propagation at a precise distance by changing the temperature over a narrow range of 0.2 K. No material has enabled controllable selection of spin propagation length so far. Therefore, the application of magnetofermionic condensate for spin transfer opens up new opportunities for the manipulation of the spin degree of freedom in solids. It becomes even possible to create a temperature-controlled spin gates and design the spin transistor devices.

[1] J. Bass and W. P. Pratt Jr, J. Phys.: Cond. Matter 19, 183201, (2007)
[2] C. Kallin and B. I. Halperin, Phys. Rev. B., 30, 5655 (1984)
[3] L. V. Kulik, A. V. Gorbunov, A. S. Zhuravlev, V. B. Timofeev, S. Dickmann and I. V. Kukushkin, Sci. Rep., 5, 10354, (2015)
[4] L. V. Kulik, A. S. Zhuravlev, S. Dickmann, A. V. Gorbunov, V. B. Timofeev, I. V. Kukushkin and S. Schmult, Nat. Commun., 7, 13499, (2016).

Exchange mediated compressible stripes in the integer quantum Hall effect regime: A possible need for a new interpretation even after 25 years

J. Oswald[1] and R.A. Römer[2]

[1]*Institute of Physics, Montanuniversität Leoben, Franz Josef Str. 18, 8700 Leoben, Austria*

[2]*Department of Physics and Centre for Scientific Computing, University of Warwick, Coventry CV4 7AL, UK*

In their pioneering work Chklovskii, Shklovskii and Glazman (CSG) addressed the local nature of edge channels [1]. Instead of narrow channels they get almost macroscopically wide compressible stripes (CS) that result from the electrostatic interaction based on Thomas-Fermi screening. Using a numerical, laterally resolved, self-consistent Hartree Fock (HF) approximation we have most recently shown [2,3] that the well-known existence of an exchange enhanced Zeeman splitting is not compatible with the existence of wide regions of partly filled Landau levels (LL). We have demonstrated that many particle interactions lead to Hund's rule-type behavior that counteracts a situation of simultaneously existing partly filled spin-up and spin-down LLs. Instead, the electron system undergoes a transformation to a mixture of clusters of full and empty LLs. A continuous change of the total filling factor either by adding/removing electrons or changing the magnetic field leads to growing or shrinking clusters of fixed density. The boundaries of these clusters remain the only compressible parts of the electron system and thus they serve as transmitting channels for transport. On the microscopic level the many body interactions act towards re-establishing narrow channels of almost non-interacting single electrons, which seems to be at variation with the CSG picture. This is in line with some of the most successful quantum Hall physics (e.g. the scaling theory), which is also based on models that rely on networks of narrow quantum channels such as the Chalker-Coddington network model [4].

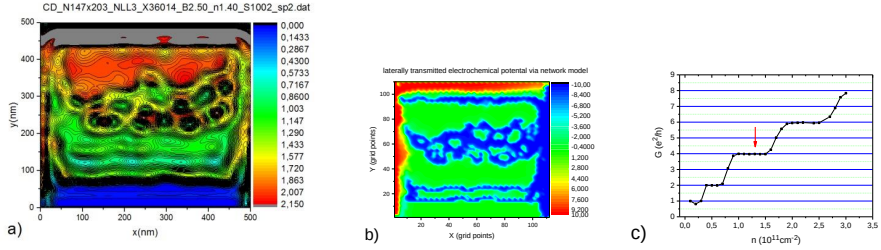

FIG.1. (a) Local filling factor distribution of spin-down electrons in the edge region as obtained by the HF calculation; the stripe of a partly filled 2nd LL is represented by a mixture of clusters of full and empty 2nd LL, that create a network of transmitting channels; (b) lateral distribution of the injected non-equilibrium chemical potential for transport. At the position of the CS (edge potential terrace) a network of "micro-channels" appears according to our non-equilibrium network model. The clockwise transmitted "blue" channels dissolve when arriving at the oppositely injected "red" potential. The vanishing bulk region is located close to the upper boundary, which can be understood to act as a hard wall potential; (c) two-point conductance as a function of electron density at fixed B=2.5T according to our non-equilibrium network model. The missing bulk region in the simulation might be responsible for the missing spin-splitting in transport, while spin-resolved edge stripes might still appear at the soft edge towards the lower boundary of the structure;

We propose a new view of the wide CS of CSG based on our most recent results. In Fig.1 we show preliminary results for simulating just the edge region on one side of a Hall bar by using a large soft bare potential of about 1000 mV for the lower edge, while the opposite (upper) edge serves as a hard wall potential. Additionally a random disorder potential of several mV amplitude is superimposed. Due to the modification of screening by just varying the size of the clusters of fully filled LLs at constant density, a Thomas-Fermi like screening behavior (like assumed by CSG) recovers only on larger length scales of several hundred nanometers well above the typical cluster size. In contrast, the details of random potential fluctuations of a size equal or less than the typical cluster size remain almost unscreened. Due to the appearance of electron clusters of varying size, the on average homogeneously looking wide CS get an internal fine structure that creates a dense network of narrow channels which maintains the transport. This can be seen in Fig.1a by the yellow colored regions that indicate narrow half-integer stripes [2,3] at the boundaries of the clusters of the half-filled 2nd spin-down LL. The fully filled 2nd spin-down LL is colored in red and the empty 2nd spin-down LL is colored in green. In Fig.1b the transmitted non-equilibrium chemical potential obtained by our network model is shown, which follows the yellow regions of Fig.1a. The spin-down LL creates one wide stripe and one narrow channel, while the not shown spin-up LL creates 2 narrow channels that leads in total to 4 channels and the plateau as marked in Fig.1c by the red arrow. In order to deal with the required computing power for a whole macroscopic sample including bulk region a suitable multiscale approach for the Hartree-Fock model has to be developed, which is the topic of future work.

[1] D. B. Chklovskii, B. I. Shklovskii and L. I. Glazman, *Phys. Rev. B*, **46,** 4026 (1992)
[2] J. Oswald and R. A. Römer, EPL (Europhysics Letters) **117**, 57009 (2017)
[3] J. Oswald and R. A. Römer, PHYSICAL REVIEW B **96**, 125128 (2017)
[4] J. T. Chalker and P. D.Coddington, *J. Phys. C: Solid State Phys.*, **21,** 2665 (1988)

Landau level spectroscopy of HgTe/CdHgTe QWs in high magnetic fields up to 34 T

L.S.Bovkun,[1,2] A.V.Ikonnikov,[1,3] K.V.Maremyanin,[1] V.Ya.Aleshkin,[1] N. N. Mikhailov,[4] S. A. Dvoretskii,[4] B.A.Piot,[2] M.Potemski,[2] M.Orlita[2] and V. I. Gavrilenko[1]

[1] *Institute for Physics of Microstructures RAS, Nizhny Novgorod, Russia*

[2] *Laboratoire National des Champs Magnétiques Intenses, LNCMI-CNRS-UGA-UPS-INSA-EMFL, Grenoble, France*

[3] *Faculty of Physics, M.V. Lomonosov Moscow State University, Moscow, Russia*

[4] *Institute of Semiconductor Physics, Siberian Branch RAS, Novosibirsk, Russia*

HgTe/CdHgTe quantum wells (QWs) with inverted band ordering attract much attention as 2D topological insulators. Magnetospectroscopy in far and mid IR range is a powerful tool to reveal the real band structure. However, to the present such studies by means of Fourier-transform spectroscopy were restricted by fields of 11 to 15 T [1-4] and only few experiments with monochromatic radiation sources were performed in pulsed magnetic filed up to 45 T [5,6]. In the present work we have performed detailed magnetospectroscopy studies in stationary magnetic fields up 34 T both in single and double HgTe/CdHgTe QWs. In the latter case new topological phases such as “bilayer graphene” and “double inversion” ones have been demonstrated. Fig.1&2 exemplify new results obtained on single QWs.

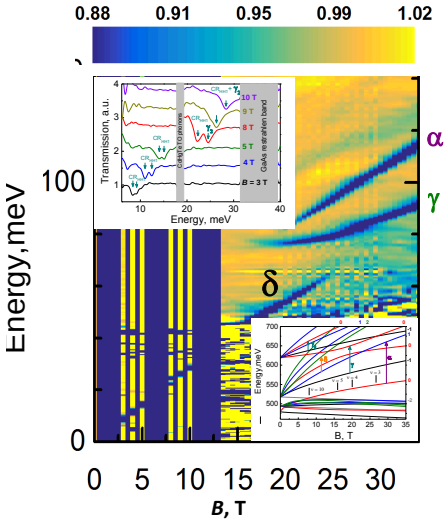

FIG. 1. Magnetotransmission spectra in single-side selectively doped QW with giant (30 meV) Rashba spin splitting at $B = 0$ [7] manifested itself as a prominent cyclotron resonance line splitting in “classical”magnetic fields up to 8 T (upper insert). At higher fields the magnetic quantization in nonparabolic conduction band dominates over Rashba splitting giving rise to α, γ and δ lines originating and decaying in accordance with Landau level filling factor ν (lower insert). A characteristic bending of the γ line results from the anticrossing behavior of Landau levels $n = 0$ in 1st and 2nd conduction subbands.

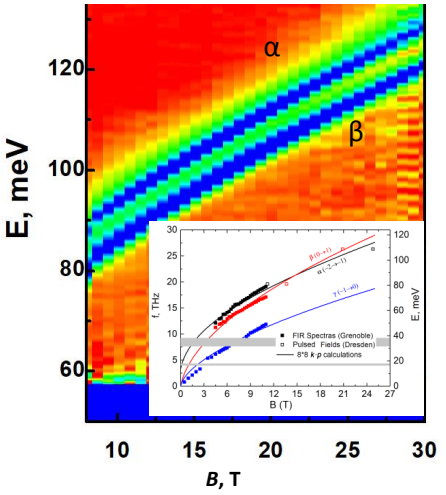

FIG. 2. Crossing avoiding of the magnetoabsorption lines α and β in HgTe/CdHgTe QW 7 nm wide [3] predicted by single particle calculations within 8-band Kane model at B ~ 16 T (see insert). The effect seems to result from the interaction of these two optical transitions.

[1] M. Schultz et al. Phys. Rev. B, 57, 14772, (1998)
[2] M. Orlita et al. Phys. Rev. B, 83, 115307, (2011)
[3] M. Zholudev et al. Phys. Rev. B, 86, 205420, (2012)
[4] M. Marcinkiewicz et al. Phys. Rev. B, 96, 035405, (2017)
[5] A.V. Ikonnikov et al. Semicond. Sci. Technol., 26, 125011, (2011)
[6] A.V. Ikonnikov et al. Phys. Rev. B, 94, 155421, (2016)
[7] K.E.Spirin et al. JETP Lett., 92, 63, (2010).

Quantum Hall stripes: high density regime and a new feature

Michael Zudov,[1] Xiaojun Fu,[1] Qianhui Shi,[1] John Watson,[2,3] Geoffrey Gardner,[3,4] Michael Manfra,[2,3,4,5] Kirk Baldwin,[6] Loren Pfeiffer,[6] and Kenneth West[6]

[1] *School of Physics and Astronomy, University of Minnesota, Minneapolis, Minnesota 55455, USA*

[2] *Department of Physics and Astronomy, Purdue University, West Lafayette, Indiana 47907, USA*

[3] *Birck Nanotechnology Center, Purdue University, West Lafayette, Indiana 47907, USA*

[4] *School of Materials Engineering, Purdue University, West Lafayette, Indiana 47907, USA*

[5] *Station Q Purdue and School of Electrical and Computer Engineering, Purdue University, West Lafayette, Indiana 47907, USA*

[6] *Department of Electrical Engineering, Princeton University, Princeton, New Jersey 08544, USA*

Quantum Hall stripes (QHS) [1] in GaAs are usually aligned along [110] crystal direction, for yet unknown reason, but are expected to align along $[1\bar{1}0]$ when the carrier density exceeds $n_e \approx 3\times10^{11}$ cm^{-2} [2]. While an in-plane magnetic field $B_\parallel$ is expected to orient QHS perpendicular to it [2], recent experiments [3] have shown that $B_\parallel$ can also favor QHS alignment *parallel* to it. In particular, it was found that $B_\parallel$ applied parallel to QHS cannot alter their orientation above certain n_e. It is thus interesting to investigate higher density quantum wells to see (i) if QHS are aligned $[1\bar{1}0]$ and (ii) if QHS, regardless of its initial alignment, can be reoriented by $B_\parallel$.

We have studied several quantum wells with densities up to 4.3×10^{11} cm^{-2} and, surprisingly, found that QHS are still oriented along conventional [110] direction even at the highest density studied. We also found that $B_\parallel$ applied along QHS *does* render them perpendicular to it at $B_\parallel \sim 1$ T. Upon further increase of $B_\parallel$, the resistance anisotropy diminished but *no* second reorientation was detected [data at filling factor $\nu = 9/2$ are shown in Fig. 1(a)], meaning that $B_\parallel$ favors QHS perpendicular to it, as in early studies [2]. We thus conclude that high n_e alone is not a decisive factor for either abnormal native QHS orientation or their alignment with respect to $B_\parallel$.

We also report on a new feature near $\nu = 13/2$ which is manifested by a local *minimum* (cf. $\uparrow$) in the hard resistance *and* a *maximum* (cf. $\downarrow$) in the easy resistance [see Fig. 1(b)] which was observed in several samples with $n_e \sim 3\times10^{11}$ cm^{-2}. While stripe anisotropy sets in at $T \lesssim 0.1$ K, this feature emerges at $T \lesssim 50$ mK and becomes stronger with decreasing temperature. Upon application of $B_\parallel$, both local extrema quickly decay and disappear at $B_\parallel \lesssim 1$ T. Remarkably, during this decay, R_{xx} at $\nu = 13/2$ is more than *doubled* while R_{yy} becomes immeasurably small. Interestingly, the feature disappears in a very similar way with increasing T; the resistance anisotropy at $\nu = 13/2$ substantially *grows* as T is raised. While the origin of this new feature remains unclear, it might be another manifestation of the recently reported nematic to smectic phase transition [5].

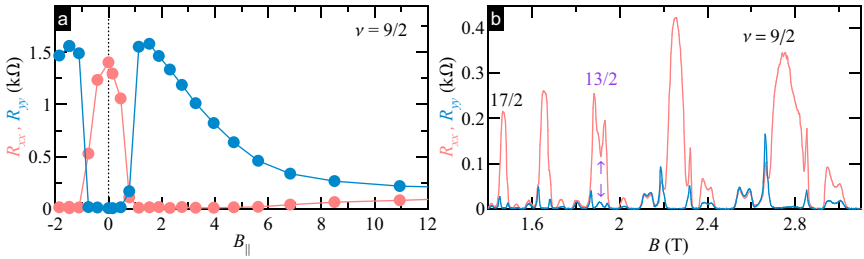

FIG. 1. *(a) R_{xx} and R_{yy} vs. $B_\parallel$ at $\nu = 9/2$ in a 24 nm-wide quantum well with $n_e \approx 4.1\times10^{11}$ cm^{-2}. (b) R_{xx} and R_{yy} vs. B in a 30 nm-wide quantum well with $n_e \approx 3.1\times10^{11}$ cm^{-2}.*

[1] A. A. Koulakov, M. M. Fogler, and B. I. Shklovskii, Phys. Rev. Lett. **76**, 499 (1996); M. P. Lilly *et al.*, Phys. Rev. Lett. **82**, 394 (1999); R. R. Du *et al.*, Solid State Commun. **109**, 389 (1999).
[2] J. Zhu *et al.*, Phys. Rev. Lett. **88**, 116803 (2002); K. B. Cooper, *et al.*, Phys. Rev. Lett. **92**, 026806 (2004).
[3] W. Pan *et al.*, Phys. Rev. Lett. **83**, 820 (1999); M. P. Lilly *et al.*, Phys. Rev. Lett. **83**, 824 (1999); T. Jungwirth *et al.*, Phys. Rev. B **60**, 15574 (1999); T. D. Stanescu *et al.*, Phys. Rev. Lett. **84**, 1288 (2000).
[4] Q. Shi *et al.*, Phys. Rev. B **93**, 121411(R) (2016); *ibid.* **95**, 161303(R) (2017).
[5] Q. Qian *et al.*, Nature Commun. **8**, 11536 (2017).

Parafermions and Majorana fermions in domain walls of quantum Hall ferromagnets

T. Wu,[1] Z. Wan,[1] A. Kazakov,[1] Y. Wang,[1] G. Simion,[1] J. Liang,[1] K.W. West,[2] K. Baldwin, [2] L.N. Pfeiffer, [2] T. Wojtowicz,[3] Y.B. Lyanda-Geller,[1] and L.P.Rokhinson,[1]

[1] *Department of Physics and Astronomy, Purdue University, West Lafayette, IN 47907 USA*
[2] *Department of Electrical Engineering, Princeton University, Princeton, NJ 08540 USA*
[3] *International Research Centre MagTop, Aleja Lotnikow 32/46, PL-02668 Warsaw, Poland*

Non-abelions in solid state systems, such as Majorana fermions, parafermions or Fibonacci anyons, must result in topologically degenerate ground state characterized by non-Abelian braiding statistics. Edges of quantum Hall systems in the presence of superconducting coupling can potentially host non-Abelions. Recently, signatures of Majorana modes were experimentally observed in quantum wires; however, the results can be also attributed to effects other than Majorana fermions. The experimental challenge in wires is that chiral spin-orbit states, which must be the cause of Majorana modes, have not been observed directly in studied samples, and that multi-mode character of quantum wires proximity coupled to superconductors and disorder bring additional complications. Chiral edges in the quantum Hall systems are single modes, creating a viable route to overcome these challenges. Most importantly, quantum degeneracy of the fractional quantum Hall effect edge states paves the way to higher order non-Abelions, such as parafermions and Fibonacci anyons, which are crucial for topological fault-tolerant quantum computing.

Early proposals for observation of non-Abelions in the quantum Hall systems proximity coupled to superconductors considered g-factors of opposite sign affecting counter-propagating edge channels. Here we describe our experimental observations and theory of electrostatically induced single domain walls at the boundary between polarized and unpolarized domains formed in the spin transitions in the integer (IQHE) and fractional (FQHE) quantum Hall effects.

In FQHE we experimentally demonstrate formation of helical conducting channels at the electrostatically induced boundaries between an incompressible polarized and unpolarized regions at filling factor $\nu = 2/3$ in a GaAs triangular quantum well. These helical channels are formed from the two counter-propagating $\nu = 1/3$ states with opposite spin. Theoretically we use field-theoretical and numerical approaches to calculate electrostatically induced FQHE edges and show that emerging domain walls have the prerequisite helical structure to support parafermion excitations when coupled to an s-wave superconductor. Experimentally demonstrated local electrostatic control of polarization allows formation of a reconfigurable network of fractional helical domain walls with fractionalized charge excitations and, potentially, parafermion braiding.

In IQHE we investigate a quantum Hall ferromagnet in Mn doped CdTe quantum wells at $\nu = 2$. We demonstrate local electrostatic control of the emerging single helical domain wall at the ferromagnetic transition. We show experimentally and theoretically that impurities play considerable role in transport through domain walls, in which spin-orbit interactions create a spectral gap. Theory of short-range impurity states and smooth random potential in spin-orbit coupled Landau levels is proposed. We demonstrate that impurities are crucial for generating Majorana modes, when gapped IQHE ferromagnetic domain wall is coupled to an s-superconductor.

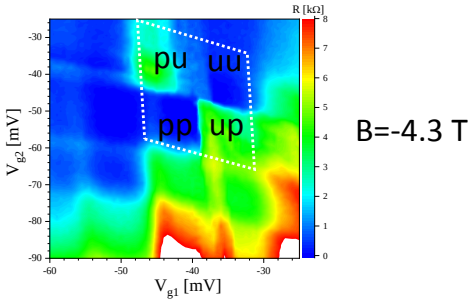

FIG. 1. Experimental demonstration of a single domain wall at the fractional quantum Hall spin transition. Measured resistance R in GaAs quantum well across the boundary formed by two gate voltages Vg1 and Vg2. Magnitude of resistance is defined by a contrast scale on the right. The region where $\nu=2/3$ under both gates is marked by a white square. Letters u and p mark unpolarized and polarized $\nu=2/3$ regions under gates. Nonzero R in (up) and (pu) quadrants indicate formation of conducting domain walls between polarized and unpolarised regions. Lithographical length of the gate boundary is 7 μm.

Magneto-transport of 2DEGs ultrastongly coupled to vacuum fields - probed by weak microwave irradiation

F. Appugliese ,[1] G. L. Paravicini Bagliani,[1] G. Scalari ,[1] E. Richter,[1] J. Keller ,[1] M. Beck,[1] and J. Faist[1]

[1]*Institute for Quantum Electronics, ETH Zurich, Zurich 8093, Switzerland*

The Ultrastrong light-matter coupling regime is predicted to alter the ground state of an electronic system [1,2]. In order to achieve this regime we use GaAs/AlGaAs Hall bars inside a microwave cavity [2]. The resonant photons in the cavity couple with the electrons at the Fermi level, which are contributing to transport.
We developed a new experimental platform, which allows us to investigate the peculiarities of Ultra strong coupling in the matter part of the polariton state. We are able to probe different electronic states (e. g. Extended and localized states), that can not be resolved in the usual optical experiments. We weakly illuminate the sample at 100 mK by means of a widely tunable single frequency sub-THz source (50-500 GHz) and we measure the change in the longitudinal magnetoresistance $\Delta\rho_{xx}$ due to the creation of mixed light-matter quasi-particles (polaritons).

In figure 1 we show the differential magnetoresistance normalized to input power as a function of magnetic field and irradiation frequency.
We observe a strong dependence of the response on the filling factor.
The magnetoresistance is reduced at half integer filling factors and this reduction shows a dependence on the irradiation frequency. This resembles the expected dispersion for the magneto plasmon polaritons.
Our microwave cavity is a $\lambda/2$ resonator with a frequency of 200 GHz (red line in figure). In green is shown the magneto plasmon (MP) dispersion; by etching the hall bar, we introduce a plasma frequency that modifies the cyclotron dispersion [3].The electric field across the Hall Bar coupled with the MP results in the MPpolariton dispersion (magenta lines).
Hence at half integer filling factor we recover the MPP dispersion with a coupling strength of Ω/ω_{cav}=20%.
At integer filling factors so at the localized states we see a different dispersion, showing that these states are not contributing to the polaritons.

As an outlook, we are developing a method to manipulate the vacuum field in situ, in order to investigate the effect of vacuum fields on QHT in complete absence of probing photons.

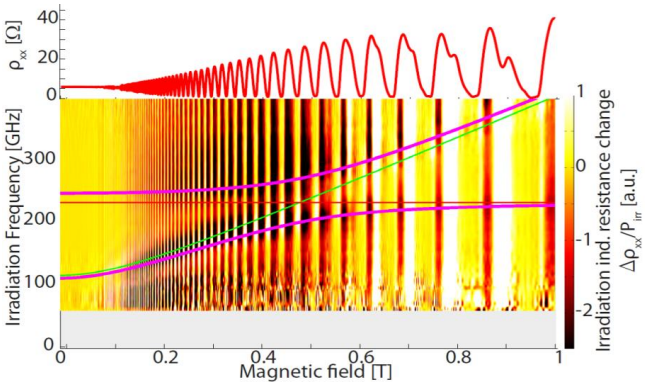

FIG. 1. Colormap: Radiation induced longitudinal resistance change Δρxx as function of irradiation frequency and magnetic field of a Hall bar inside a microwave cavity. The expected MP-polariton dispersions (magenta) result from the anti-crossing of the MP (green) and cavity (red) dispersions.[4]

[1] D. Hagenmüller et al., Phys. Rev. B, 81, 235303 (2010)
[2] G. Scalari et al., Science 335, 1323 (2012)
[3] G. Paravicini-Bagliani et al., Phys. Rev. B 95, 205304 (2017)
[4] G. Paravicini-Bagliani et al., in preparation

Competing Fractional Quantum Hall and Electron Solid Phases in Graphene

Shaowen Chen,[1,2] Rebeca Ribeiro-Palau,[1,3] Kang Yang,[4,5] K. Watanabe,[6] T. Taniguchi,[6] James Hone,[3] Mark O. Goerbig,[5] and Cory R. Dean[1]

[1]*Department of Physics,* [2]*Department of Applied Physics and Applied Mathematics,* [3]*Department of Mechanical Engineering, Columbia University, New York, New York 10027, United States*

[4]*Laboratoire de Physique des Solides,CNRS UMR 8502,, Université Paris-Sud, Orsay cedex 91405, France*

[5]*LPTHE, CNRS-Université Pierre et Marie Curie, Sorbonne Universités, 4 Place Jussieu, 75252 Paris Cedex 05, France*

[6]*National Institute for Materials Science, 1-1 Namiki, Tsukuba, Japan*

Partially filled landau levels (LL) host a variety of collective ground states that generally fall into two classes: fractional quantum Hall (FQH) liquids, and electron solids. In the lowest landau level of GaAs these phases generically compete, giving rise to a reentrant integer quantum Hall effect (RIQHE), where in between the FQH plateaus, pinning of the electron solid phase causes the Hall resistance to deviate from its classical value and return to the nearest integer value. While the integer and FQH effect has now been reported in a wide variety of 2D electron systems, observation of the RIQHE as evidence of the electron solid phase, has only been seen in high quality GaAs/AlGaAs quantum wells [1]. Recently, an analogous RIQHE was predicted [2] to be the low energy ground state near 1/3 filling in the N=2 LL of graphene, however experimental evidence has not been forthcoming. Here, using a dual-gate architecture to fabricate ultra-high mobility graphene with widely tunable carrier density we report the first experimental confirmation of the RIQHE in monolayer graphene, appearing in the N=2 LL at fields in excess of 15 T. The tunability of graphene carrier density allows us to fully study the evolution of this reentrant state in both magnetic field and temperature, allowing us to construct the first *B-T* phase diagram at fixed filling fraction for the electron solid phase.

At high magnetic field, we observed reentrant states accompanied by FQH states at partial filling 1/5, as shown in figure 1A. There is a minimum field where the FQH state is strengthened and the usual RIQHE signature emerges. Interestingly, this signature is not observed near $\upsilon = 7$, which suggests electron-hole symmetry is broken. The evolution of the RIQHE in temperature reveals the melting point of electron solid, which was measured under different magnetic field. The phase boundary of the electron solid in Figure 1C reflects a linear dependence on magnetic field, which can be explained by a dipolar energy scale expected in our double gated device. At low magnetic fields, the $\upsilon = 6$ integer plateau extends over $\upsilon = 6\frac{1}{5}$, indicating an inversion of ground state order where FQH liquid gives way to electron solid (Fig. 1B).

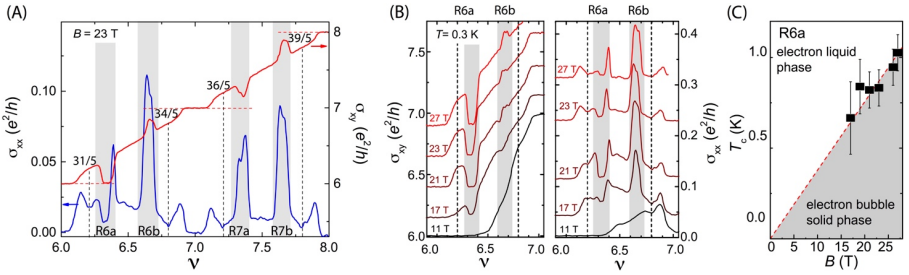

FIG. 1. (**A**) Competing Laughlin liquid and electron solid phases in N = 2 Landau level of graphene displayed as RIQHE. (**B**) Magnetic field evolution of the RIQHE (**C**) the first phase diagram for electron solid phase.

[1] Eisenstein, et al. *PRL* 7, 88 (2002).
[2] Knoester, et al. *PRB* 15, 93 (2016).

Study of nodal-line Dirac semimetal ZrSiS along *c*-direction by angular-magnetoresistance and mapping of the Q2D Fermi pocket

Mario Novak,[1] Filip Orbanić,[1] Nikola Biliškov,[2] Toshihito Osada,[3] Kazuto Uchida,[3] Mitsuyuki Sato,[3] and Ivan Kokanović[1,4]

[1] *Department of Physics, Faculty of Science, University of Zagreb, Croatia,*
[2] *Ruđer Bišković Institute, Zagreb, Croatia,*
[3] *The Institute for Solid State Physics, The University of Tokyo, Kashiwa, Japan,*
[4] *Cavendish Laboratory, University of Cambridge, Cambridge, United Kingdom*

For the first time to our knowledge, we present c-axes angular magnetoresistance study of ZrSiS, a nodal-line 3D Dirac semimetal which has recently attracted a lot of attention.[1,2,3] In ZrSiS the valence and conduction band are touching along a line in *k*-space thus forming a line node. Which gives rise to a number of new physical phenomena.

Optimisation of crystal growth allowed us to grow samples of considerable thickness to perform the *c*-direction transport measurements. We have found the low-temperature anisotropy of a factor of 30 between the *ab*-plane and *c*-direction resistivity. Moreover, angular magnetoresistivity (AMR) shows very pronounced dependence on the direction of the magnetic field in polar and azimuthal direction, resembling the AMR observed in organic Q2D materials. This peculiar AMR suggests that the Q2D Fermi pocket seen by the quantum oscillations in dominant in the AMR, and other pockets give just background signal. From the shape of AMR, we manage to reconstruct the main features of the Q2D Fermi pocket. This pocket has a strong signal in the quantum oscillations but cannot be detected by the angle-resolved photoemission measurements (ARPES). The AMR reveals coherence-peak-like feature and third-angle-like feature often seen in Q2D organic conductors.

We believe our new finding is significant for full understanding the magnetotransport in this material. Our data could be used for explaining the unusual (unique) butterfly shaped magnetoresistivity found in this material.[2]

[1] L. M. Shoop, *et* al. Nature Communications **7**, 11696 (2016).
[2] M. Z. Ali, *et* al, Science Advances **2**, e1601742 (2016).
[3] J. Hu, *et* al. Phys. Rev. Lett. **117**, 016602 (2016).

	Sunday 22 July	Monday 23 July	Tuesday 24 July	Wednesday 25 July	Thursday 26 July	Friday 27 July
8h50		Opening				
9h00		P. Kim	N. Hussey	M. Yankowitz	T. Heinz	B. Béri
9h30		T. Szkopek	L.E. Golub	C. Dean	A. Arora	Lyand-Geller
9h45		M.V.Durnev	T. Khouri	L.Lzulakowska	J. Holler	F.Appugliese
10h00		J. Lau	D. Smirnov	B.Urbaszek	A. Mitioglu	S. Chen
10h15		E. Henriksen	S.Wiedmann	M.R. Molas	Slobodeniuk	M. Novak
10h30		Coffee break				
11h00		A. Young	A. Coldea	N. Wang	G. Gusev	L. Weiss
11h30		Y. Zhang	P. Sessi	M. Glazov	A. Suslov	O.Makarovsky
1200		Buffet Lunch	Buffet Lunch	Conference Excursion with packed lunch	Buffet Lunch	Closing
14h00		G. Yusa	R.McDonald		A. Surrente	
14h30		B. Fauqué	T. Story		A. Akrap	
15h00		T. Taen	K.S.Denisov		M. Naumann	
15h15		N. Han Tu	F. Telesio		Shahrokhvand	
15h30		X. Liu	K. Rubi		D.K. Efetov	
15h45		S. Crooker	R.Masutomi		F.Parmentier	
16h00		Coffee	Coffee		Coffee	
16h30		Shot gun 1 + Poster Session Mo + Cocktail dinatoire	Shot gun 2 + Poster Session Tu + Cocktail dinatoire		A.Gorbunov	
16h45					J. Oswald	
17h00					V.Gavrilenko	
17h15					M. Zudov	
17h30						
18h00	Welcome reception NOVOTEL					
20h00				Reception/ Banquet		
21h00						